

Centre Eau Terre Environnement

Évolution du régime des précipitations au sud de Québec

Par

Wiem Rjeb

Mémoire ou thèse présentée pour l'obtention du grade de
Maître ès Sciences (M.Sc.) en sciences de la terre

Jury d'évaluation

Président du jury et
examinateur interne

André St-Hilaire
INRS-ETE

Examinateur externe

Nizar Bouguila
Institut d'ingénierie des systèmes
d'information de Concordia

Directeur de recherche

Taha B.M.J. Ouarda
INRS-ETE

AVANT-PROPOS

Ce mémoire de maîtrise par article est composé de deux parties. La première partie intitulée << SYNTHÈSE >>, inclut un résumé de la problématique, des méthodes utilisées et des résultats obtenus. La deuxième partie est constituée d'un article scientifique produit où les méthodes théoriques et les résultats sont détaillés.

Le titre et les auteurs de l'article sont :

Titre: Precipitation variability in southern Quebec and its teleconnections with global climate indices.

Auteurs : Wiem Rjeb, Taha B.M.J. Ouarda

REMERCIEMENTS

Tout d'abord, je vais commencer par me remercier pour tous les efforts accomplis durant cette maîtrise, pour ne pas lâcher et surmonter toutes les difficultés rencontrées, en particulier en pleine pandémie.

Ensuite, je vais remercier ma compagne Khaoula Laazibi pour l'amour, l'encouragement et la foi en mes accomplissements m'ayant permis de renforcer ma détermination. Je voudrais également remercier ma famille. Je suis ici aujourd'hui grâce à vos efforts innombrables.

Un grand merci pour mon encadrant et mon mentor Taha Ouarda, qui a donné une direction à ce travail grâce à ses conseils et sa disponibilité.

Mes amies Zina, Alice, Nadia et Ophélie, ma gratitude vous revient également, pour ces moments où j'avais besoin de m'évader, d'être soutenue et épaulée.

À toutes les personnes qui ont contribué à l'aboutissement de ce travail et à sa réussite, merci d'avoir donné vie à ce projet !

RÉSUMÉ

L'analyse de la variabilité des précipitations fait l'objet de nombreux travaux de recherche. La bonne caractérisation de cette variable hydrologique est nécessaire pour mieux estimer le risque associé à la conception et au dimensionnement des ouvrages hydrauliques, pour réduire les pertes financières et humaines dans les cas des inondations et celles associées à la faune et la flore dans le cas de la sécheresse.

Le Québec, la seconde région qui reçoit la plus grande quantité de neige (entre 200 et 300 cm) en Amérique du nord, présente des risques d'inondations à cause de la fonte de neige hivernale qui génère des crues printanières. Cette province produit la grande majorité de son électricité à partir du potentiel hydroélectrique. En effet, L'hydroélectricité représente près de 97% de toute l'énergie électrique produite dans cette région.

Aujourd'hui, plusieurs études ont signalé les interactions qui pourraient exister entre les indices d'oscillation climatique de basse fréquence et les variables hydro-climatologiques associées. Ces oscillations climatiques portent les signaux de la variabilité dans la circulation atmosphérique et océanique et permettent de quantifier l'évolution temporelle d'un processus climatique pour une région particulière.

L'objectif de ce projet de recherche est d'étudier la variabilité interannuelle des précipitations totales annuelles et maximales dans le sud du Québec et d'examiner les liens entre ces dernières et les indices climatiques à basse fréquence à travers une analyse de corrélation et une analyse spectrale en ondelettes.

Les résultats montrent que les précipitations annuelles, totales est maximales, sont dominées par trois modes climatiques ; l'Oscillation Arctique « Arctic Oscillation (AO) », l'Oscillation de l'Atlantique du Nord (version de Jones, 1997) « North Atlantic Oscillation Jones version (NAOj) » et l'oscillation Tropicale de l'Atlantique Nord « Tropical Northern Atlantic index (TNA) ». La considération ces derniers dans les modèles de prévision à long terme des précipitations dans le sud du Québec devra améliorer l'estimation des précipitations.

Mots-clés : Téléconnexions, Indices climatiques, Variabilités des précipitations, Québec, Analyse en ondelettes, Méthodes de détections baysiennes, Analyse de tendances.

TABLE DES MATIÈRES

AVANT-PROPOS	III
REMERCIEMENTS	IV
RÉSUMÉ	V
TABLE DES MATIÈRES	VII
LISTE DES ABRÉVIATION	IX
CHAPITRE 1 : SYNTHÈSE	1
1. INTRODUCTION.....	2
1.1 MISE EN CONTEXTE	2
1.2 PROBLEMATIQUE	3
1.3 OBJECTIFS	3
1.4 ORIGINALITÉ.....	4
1.5 ORGANISATION DE LA SYNTHÈSE	4
2. MÉTHODES.....	5
2.1 ANALYSE DE LA TENDANCE	5
2.2 MÉTHODE DE DÉTECTION DE POINTS DE CHANGEMENT.....	5
2.3 ANALYSE DE CORRÉLATION.....	6
2.4 ANALYSE EN ONDELETTES.....	6
3. ZONE D'ÉTUDE	7
4. RÉSULTATS.....	8
5. CONCLUSIONS ET PERSPECTIVES	9
6. REFERENCES.....	10
CHAPITRE 2: PRECIPITATION VARIABILITY IN SOUTHERN QUEBEC AND ITS TELECONNECTIONS WITH GLOBAL CLIMATE INDICES.....	14

LISTE DES ABRÉVIATION

AMO : Atlantic Multidecadal Oscillation

AO : Arctic Oscillation

CWT : Continuous Wavelet Transform

EA : East Atlantic

ENSO : El Niño Southern Oscillation

JFM : Janvier-Février-Mars

NAO : North Atlantic Oscillation

NAO_J : North Atlantic Oscillation (Jones)

OND : Octobre-Novembre-Décembre

PC : Point de changement

PDO : Pacific Decadal Oscillation

PNA : Pacific North American

SOI : Southern Oscillation Index

TNA : Tropical Northern Atlantic

WA : Wavelet Analysis

WHWP : Western Hemisphere warm pool

WTC : Wavelet Transform Coherence

XWT : Cross Wavelet Transform

CHAPITRE 1 : SYNTHÈSE

1. INTRODUCTION

1.1 Mise en contexte

L'amélioration de la caractérisation des précipitations actuelles et futures est essentielle à la conception des ouvrages hydrauliques, à la gestion des ressources en eau ainsi qu'à la réduction des pertes financières et humaines causées par les inondations et les sécheresses. Les précipitations, principal moteur du cycle hydrologique, sont caractérisées par une variabilité spatiale et temporelle naturelle, qui est amplifiée par le réchauffement climatique. Le rapport actuel du Groupe d'experts intergouvernemental sur l'évolution du climat (GIEC) montre que les précipitations ont augmenté sur les zones nordiques (au-dessus de 30° N) depuis le début de l'enregistrement jusqu'au milieu des années 1970 et ont progressivement diminué par la suite (Trenberth et Fasullo 2007).

Le Québec, qui est la région d'Amérique du Nord qui reçoit la deuxième plus grande quantité de neige (entre 200 et 300 cm par an en moyenne) après les Rocheuses (Dorsaz et Brown 2008), est exposée à des risques d'inondation en raison de la fonte des neiges hivernales qui entraîne des crues au printemps (Assani et Tardif 2005, Larocque et al. 2010, Nastev et al. 2005, Boucher et al. 2011, Ouarda et al. 2001). De plus, le Québec produit la majorité de son électricité à partir de sources hydrauliques. En effet, l'hydroélectricité représente près de 97% de l'énergie électrique consommée dans la région.

Les séries temporelles de différents processus hydrologiques présentent certains types de variabilité comme la tendance, la variation cyclique et la dépendance avec d'autres variables explicatives dites covariables. Aujourd'hui les indices d'oscillations climatiques de basse fréquence sont fréquemment utilisés comme covariables dans le développement des modèles non-stationnaires de prévision des précipitations. Dans ce cadre, plusieurs auteurs ont évalué les interactions qui pourraient exister entre les indices climatiques et leurs variables hydro-climatologiques associées. Ces oscillations climatiques portent les signaux de la variabilité dans la circulation atmosphérique et océanique (Goly & Teegavarapu, 2012 ; Rossi et al., 2011 ; Seierstad et al., 2007) et permettent de quantifier l'évolution temporelle d'un processus climatique pour une région particulière (Lee et al., 2013).

La présente étude a été conçue pour évaluer la tendance des séries chronologiques de précipitations sur le sud du Québec en utilisant une version modifiée du test original de Mann-Kendall (MK), qui tient compte de la corrélation sérielle. Le test de tendance de Mann-Kendall (Kendall et Stuart 1967, Mann 1945) est l'un des tests les plus utilisés pour détecter les tendances dans les séries chronologiques hydrologiques et climatologiques (Zhang et al. 2001, Fiala et al., 2010).

En outre, la présence de changements soudains dans les séries chronologiques de précipitations a été étudiée à l'aide d'une procédure bayésienne de détection de points de changement multiples (Seidou et al. 2007). Puisque les oscillations climatiques peuvent affecter l'évolution observée des extrêmes de précipitations, le deuxième objectif de la présente étude est d'identifier les indices climatiques régionaux montrant des relations significatives avec les précipitations annuelles totales et maximales dans le sud-est du Québec en utilisant l'analyse de corrélation et d'explorer les interactions sur une plage de temps-fréquence entre les précipitations du sud du Québec et certains indices climatiques en utilisant l'analyse par ondelettes. À l'échelle mondiale, l'analyse en ondelettes est largement utilisée dans diverses études de recherche, surtout lorsqu'il s'agit d'analyser les événements de précipitation et leur téléconnection avec le climat mondial (Canchala et al. 2020, Hermida et al. 2015, Jiang et al. 2014, Tan et al. 2016), ainsi que les modèles de précipitation saisonniers et mensuels (Aguilar et al. 2005, Chandran et al. 2016, Fritier et al. 2012, Kim 2004, Pathak et al. 2016, Wang et al. 2017).

1.2 Problématique

Les modèles linéaires classiques ne peuvent pas fournir une représentation adéquate de la variabilité des précipitations. De plus, les modèles non linéaires développés ne prennent pas en compte les relations entre cette variable hydrologique et les schémas à grande échelles d'anomalies de pression et de climats. L'intégration des indices climatiques dans les modèles de prévision saisonnière à long-terme peut améliorer la performance et l'efficacité de ces derniers.

1.3 Objectifs

L'Objectif de cette étude est d'étudier la variabilité interannuelle des précipitations totales annuelles et maximales dans le sud de Québec et d'examiner les liens entre ses dernières et les indices climatiques pour éventuellement les utiliser comme principaux prédicteurs dans les modèles de prévisions saisonniers.

1.4 Originalité

Il n'existe pas assez d'études sur la variabilité spatio-temporelle des précipitations depuis la décennie 1970 au Québec et les études réalisées ont analysé la variabilité des précipitations seulement à court terme. La présente étude est exhaustive (considère tous les indices climatiques possibles) et considère, pour chaque indice, le délai optimal pour maximiser le pouvoir prédicteur de l'indice.

1.5 Organisation de la synthèse

La présente synthèse est divisée en cinq sections principales. La section 1 présente l'introduction. La section 2 explique les méthodes utilisées. La section 3 fournit des renseignements sur la zone d'étude ainsi que les variables utilisées. La section 4 résume les principaux résultats. La section 5 présente les conclusions et les perspectives de l'étude.

2. MÉTHODES

Le principe et les équations de base de chaque approche utilisée dans cette étude sont présentés et détaillés dans l'article. Un résumé de chaque méthode statistique utilisée est présenté dans les sous-sections suivantes.

2.1 Analyse de la tendance

Le test de Mann-Kendall est un test non paramétrique utilisé pour déterminer si une tendance est identifiable dans une série temporelle. Il examine deux hypothèses : l'hypothèse nulle (H_0) traduisant la stationnarité des séries chronologiques et l'hypothèse alternative (H_1) impliquant la présence d'une tendance, à la hausse ou à la baisse, au fil du temps. Le test, dans sa forme originale, peut détecter des fausses tendances lorsqu'une autocorrélation positive est détectée dans les données.

Le test de tendance de Mann-Kendall modifié est une version qui applique une correction à la variance de la statistique du test pour éliminer l'effet d'autocorrélation dans les données.

Ensuite, l'approche analyse la différence de signes entre les échantillons de données antérieurs et postérieurs. L'idée est que si une tendance est présente, les valeurs de signe auront tendance à augmenter constamment, ou à diminuer constamment. Chaque valeur est comparée à toutes celles qui la précèdent dans la série chronologique, ce qui donne un total de $n(n - 1) / 2$ paires de données, où n est le nombre d'observations dans l'ensemble.

2.2 Méthode de détection de points de changement

Lorsqu'un ou plusieurs paramètres d'un modèle statistique subit un changement significatif brusque, on parle d'un Point de Changement (PC) qui date du moment où le changement a eu lieu. Les méthodes de détection de changement basées sur les statistiques Bayésiennes permettent l'identification des multiples points des changements avec leurs ampleurs et leurs positions entre une variable de réponse et l'ensemble des variables explicatives. Elles permettent d'identifier un changement s'il y'a eu lieu, l'emplacement et le nombre de changement dans les séries chronologiques annuelles. En fournissant une distribution de probabilité a posteriori entière de la position de changement. En cas d'absence des variables explicatives, elle détecte les changements dans la série chronologique de la variable de réponse au cours du temps.

2.3 Analyse de corrélation

Le coefficient de corrélation utilisé dans cette étude est le coefficient Pearson, noté r , qui est la covariance des deux variables continues ; x et y normalisée par le produit de leurs écarts types. Le degré de signification statistique est évalué en utilisant le test t de Student en testant l'hypothèse nulle, H_0 , qui assume qu'aucune corrélation n'existe entre les deux variables x et y ($r=0$). L'hypothèse alternative, H_1 , implique qu'il existe une relation linéaire entre x et y ($r \neq 0$).

2.4 Analyse en Ondelettes

L'analyse en ondelettes permet de capturer les changements d'échelle temporelle dans et entre les séries temporelles le biais de plusieurs transformations. La périodicité des séries de précipitations est examinée en utilisant la transformée en ondelette continue (Continuous Wavelet Transform, CWT). Cette transformée permet d'identifier à la fois les modes dominants de variabilité et la manière dont ces modes varient dans le temps tout en décomposant la série temporelle cible dans l'espace temps-fréquence et en fixant l'ondelette-mère. La corrélation croisée des deux séries temporelles dans l'espace-temps-fréquence est examiné par le biais de la transformée en ondelettes croisées (Cross Wavelet Transform, XWT), permettant de détecter les régions de puissances significativement importantes dans l'espace temps-fréquence. La corrélation des deux séries temporelles dans l'espace-temps-fréquence est étudiée avec la méthode de cohérence en ondelettes (Wavelet Transform Coherence, WTC) dans le but d'identifier les régions où les deux séries chronologiques couvraient dans l'espace temps-fréquence.

3. ZONE D'ÉTUDE

L'ensemble de données utilisées dans la présente étude comprend les données des précipitations journalières de 25 stations météorologiques réparties uniformément dans le sud de la province Québec-Canada. Ces stations couvrent les trois régions hydroclimatiques homogènes identifiées dans le sud du Québec (Assani et al. (2011) : la région hydroclimatique sud-est (SE), la région hydroclimatique sud-ouest (SW) et la région hydroclimatique est (E). La région hydroclimatique du sud-est (SE) est située sur la rive droite du fleuve Saint-Laurent (rive sud), la région hydroclimatique de l'est (E) est située au nord de 47°N et la région hydroclimatique du sud-ouest (SW), principalement située sur la rive nord (rive gauche) du fleuve. À partir des données quotidiennes, les variables suivantes sont calculées : les précipitations annuelles totales et maximales, les précipitations saisonnières totales et maximales. La présente étude examine certaines des principales oscillations climatiques mondiales afin de déterminer leurs effets sur les précipitations annuelles totales et maximales dans la région sud du Québec. Les modèles climatiques à grandes échelles employés dans cette étude sont les modèles présentés dans la littérature : ENSO, NAO, AO, PDO, PNA, TNA, WHWP, EA et AMO. Ces données sont extraites des bases de données de l'Administration Nationale des Océans et de l'Atmosphère pour la période de 1952 à 2019.

4. RÉSULTATS

Avec une analyse de la tendance à long terme des précipitations sur 25 séries temporelles totales dans le sud du Québec, cette étude nous permet de conclure qu'une majorité de stations de précipitations montrent des tendances significatives à la hausse. En ce qui concerne la tendance des précipitations annuelles totales, les stations situées au sud du 47°N indiquent une augmentation. En revanche, aucune des tendances obtenues n'est statistiquement significative pour les stations situées au nord de 47°N. Lorsque nous examinons la tendance saisonnière, nous sommes en mesure de conclure qu'un nombre important de stations de précipitations connaissent des augmentations significatives pendant la saison des pluies.

Les changements brusques dans le comportement des précipitations annuelles ont été observés entre 1965-1985 et 1985-1995 pour les précipitations annuelles totales, et entre 2005-2015 pour les précipitations annuelles maximales. Ces périodes sont connues par des anomalies et des changements présentés dans les séries des indices climatiques globaux.

En outre, ce travail a proposé d'explorer la relation statistique entre les données de précipitations et plusieurs indices climatiques. Une analyse de corrélation et une analyse en ondelettes ont été effectuées sur les valeurs moyennes mobiles trimestrielles précédentes des différents modèles climatiques et des valeurs de précipitations annuelles. Les résultats de cette enquête nous ont permis de retenir trois modes climatiques dominants dans la zone d'étude : AO, NAOj et TNA. En outre, les précipitations annuelles totales ont une corrélation positive avec l'AO et une corrélation négative avec le NAOj. L'analyse montre également que les précipitations annuelles maximales sont en phase avec l'indice TNA et en opposition avec l'indice NAOj.

Les précipitations totales à l'échelle annuelle sont soumises à des cycles significatifs de deux à trois ans. Contrairement à la région de l'est, la périodicité dans les régions du sud-est et du sud-ouest est plus faible. En termes de précipitations annuelles, un cycle de 2 à 3 ans est évident. Parallèlement, les précipitations annuelles maximales présentent quatre à huit cycles significatifs.

En outre, les tracés XWT ont révélé que la relation entre les données de précipitations totales et maximales et les indices climatiques retenus dans la région orientale est plus significative que celle des régions du sud-est et du sud-ouest. Les zones de puissances les plus élevées sont détectés dans les mois où on a trouvé les plus forts coefficients de corrélation.

Les tracés WTC démontrent un haut degré de cohérence entre les indices retenus et les variables d'intérêt considérées dans cette étude dans les mêmes périodes de corrélation significative.

5. CONCLUSIONS ET PERSPECTIVES

Ce travail a exploré les liens statistiques entre les données des précipitations et plusieurs indices climatiques. Une analyse de corrélation nous a permis de retenir trois modèles climatiques dominants dans la zone d'étude, l'indice AO, NAOj et TNA. Les résultats de l'analyse spectrale en ondelettes ont permis non seulement de confirmer l'influence de ces trois indices d'oscillations climatiques sur les précipitations mais aussi d'avoir des connaissances sur les différents modes de variabilité des précipitations au sud du Québec en les combinant avec les résultats de tendances et l'analyse de corrélation. Précisément, l'influence est plus prononcée entre les indices retenus et les précipitations annuelles et maximales appuyant la nécessité de considérer ces derniers dans les modèles de prévision à long terme des précipitations dans la zone d'étude.

Dans la perspective de ce travail, les indices retenus peuvent être des prédicteurs dans les modèles de prévision non linéaire des précipitations à long terme au sud du Québec.

6. REFERENCES

Aguilar, E., Peterson, T., Obando, P.R., Frutos, R., Retana, J.A., Solera, M., Soley, J., García, I.G., Araujo, R. and Santos, A.R. (2005) Changes in precipitation and temperature extremes in Central America and northern South America, 1961–2003. *Journal of Geophysical Research:*

Assani, A. and Tardif, S. (2005) Classification, caractérisation et facteurs de variabilité spatiale des régimes hydrologiques naturels au Québec (Canada). Approche éco-géographique. *Revue des sciences de l'eau/Journal of Water Science* 18(2), 247-266.

Assani, A.A., Chalifour, A., Légaré, G., Manouane, C.-S. and Leroux, D. (2011) Temporal regionalization of 7-day low flows in the St. Lawrence watershed in Quebec (Canada). *Water resources management* 25(14), 3559-3574.

Canchala, T., Alfonso-Morales, W., Cerón, W.L., Carvajal-Escobar, Y. and Caicedo-Bravo, E. (2020) Teleconnections between monthly rainfall variability and large-scale climate indices in southwestern Colombia. *Water* 12(7), 1863.

Chandran, A., Basha, G. and Ouarda, T. (2016) Influence of climate oscillations on temperature and precipitation over the United Arab Emirates. *International Journal of Climatology* 36(1), 225-235.

Dorsaz, F. and Brown, R. (2008) Évaluation des simulations du couvert nival sur le Québec par les modèles MRCC 4.2. 3 et GEMCLIM 3.3. 0. Rapport de stage, Ouranos 49.

Fiala, T., Ouarda, T.B.M.J., and J. Hladny (2010). Evolution of low flows in the Czech Republic, *Journal of Hydrology*, 393 (2010) 206–218.

Fritier, N., Massei, N., Laignel, B., Durand, A., Dieppois, B. and Deloffre, J. (2012) Links between NAO fluctuations and inter-annual variability of winter-months precipitation in the Seine River watershed (north-western France). *Comptes Rendus Géoscience* 344(8), 396-405.

Goly, A. and Teegavarapu, R.S. (2012) Influence of teleconnections on spatial and temporal variability of extreme precipitation events in Florida, pp. 1899-1908.

Hermida, L., López, L., Merino, A., Berthet, C., García-Ortega, E., Sánchez, J.L. and Dessens, J. (2015) Hailfall in southwest France: Relationship with precipitation, trends and wavelet analysis. *Atmospheric Research* 156, 174-188.

Jevrejeva, S., Moore, J. and Grinsted, A. (2003) Influence of the Arctic Oscillation and El Niño-Southern Oscillation (ENSO) on ice conditions in the Baltic Sea: The wavelet approach. *Journal of Geophysical Research: Atmospheres* 108(D21).

Jiang, R., Gan, T.Y., Xie, J. and Wang, N. (2014) Spatiotemporal variability of Alberta's seasonal precipitation, their teleconnection with large-scale climate anomalies and sea surface temperature. *International Journal of Climatology* 34(9), 2899-2917.

Kendall, M.G. and Stuart, A. (1967) The Advanced Theory of Statistics. Population (18^e année), 396-396.

Kim, S. (2004) Wavelet analysis of precipitation variability in northern California, USA. *KSCE Journal of Civil Engineering* 8(4), 471-477.

Kumar, K.N., Molini, A., Ouarda, T.B.M.J. and Rajeevan, M.N. (2017). North Atlantic controls on wintertime warm extremes and aridification trends in the Middle East, *Scientific Reports*, 7(1): 12301.

Larocque, M., Fortin, V., Pharand, M. and Rivard, C. (2010) Groundwater contribution to river flows—using hydrograph separation, hydrological and hydrogeological models in a southern Quebec aquifer. *Hydrology and Earth System Sciences Discussions* 7(5), 7809-7838.

Lee, T., Ouarda, T.B.M.J. and Li, J. (2013) An orchestrated climate song from the Pacific and Atlantic Oceans and its implication on climatological processes. *International Journal of Climatology* 33(4), 1015-1020.

Mann, H.B. (1945) Nonparametric tests against trend. *Econometrica: Journal of the econometric society*, 245-259.

Nastev, M., Rivera, A., Lefebvre, R., Martel, R. and Savard, M. (2005) Numerical simulation of groundwater flow in regional rock aquifers, southwestern Quebec, Canada. *Hydrogeology journal* 13(5), 835-848.

Pathak, P., Kalra, A., Ahmad, S. and Bernardez, M. (2016) Wavelet-aided analysis to estimate seasonal variability and dominant periodicities in temperature, precipitation, and streamflow in the Midwestern United States. *Water resources management* 30(13), 4649-4665.

Rossi, A., Massei, N. and Laignel, B. (2011) A synthesis of the time-scale variability of commonly used climate indices using continuous wavelet transform. *Global and Planetary Change* 78(1-2), 1-13.

Seidou, O. and Ouarda, T.B.M.J (2007) Recursion-based multiple changepoint detection in multiple linear regression and application to river streamflows. *Water Resources Research* 43(7).

Seidou, O., Asselin, J.J., and T.B.M.J., Ouarda (2007). Bayesian multivariate linear regression with application to changepoint models in hydrometeorological variables, *Water Resources Research*. 43, W08401.

Tan, X., Gan, T.Y. and Shao, D. (2016) Wavelet analysis of precipitation extremes over Canadian ecoregions and teleconnections to large-scale climate anomalies. *Journal of Geophysical Research: Atmospheres* 121(24), 14,469-414,486.

Trenberth, K.E. and Fasullo, J. (2007) Water and energy budgets of hurricanes and implications for climate change. *Journal of Geophysical Research: Atmospheres* 112(D23).

Zhang, X., Harvey, K.D., Hogg, W. and Yuzyk, T.R. (2001) Trends in Canadian streamflow. *Water Resources Research* 37(4), 987-998.

**CHAPITRE 2: PRECIPITATION VARIABILITY IN SOUTHERN QUEBEC
AND ITS TELECONNECTIONS WITH GLOBAL CLIMATE INDICES.**

**Precipitation variability in southern Quebec and its teleconnections with
global climate indices.**

Wiem Rjeb¹, Taha B.M.J Ouarda¹

¹ Canada Research Chair in Statistical Hydro-Climatology, Institut national de la recherche scientifique, Centre Eau Terre Environnement. INRS-ETE, 490 De la Couronne, Québec City, QC, Canada

Octobre, 2021

This article will be submitted to the Canadian Water Resources Journal.

Abstract

This paper examines the inter-annual variability of precipitation in southern Quebec, Canada and its relationship to large-scale atmospheric circulation patterns. Long record precipitation series at 25 meteorological stations in the province of Quebec, Canada, are used to assess long-term trends and detect possible change points in maximum and total annual precipitation. Based on the modified Mann-Kendall test results, the majority of stations display significant precipitation trends at the 5% level. On an annual timescale, all significant trends are increasing. The analysis of seasonal time series reveals strong increasing trends mainly during the rainy season. According to the Bayesian change-point detection method, the majority of change points are observed between 1965-1985 and 1985-1995 for total annual precipitation, and between 2005-2015 for maximum annual precipitation. Linear correlation and wavelet analysis revealed potential effects of the Arctic Oscillation, the North Atlantic Oscillation Jones, and the Tropical Northern Atlantic Index on long-term total precipitation variability in the study area. The impact of these patterns increases from east to west.

Keywords: Precipitation; variability; teleconnections; trend; change point; Mann-Kendall test, wavelet analysis; climate index; Quebec.

1. Introduction

The characterization of present and future precipitation is essential for the design of hydraulic structures, water resource management, and the reduction of the financial and human losses caused by floods and droughts. Precipitation, the primary driver of the hydrological cycle, is characterized by natural spatial and temporal variability, which is amplified by global warming. The International Panel on Climate Change (IPCC 2012) indicated that precipitation increased over North America (above 30° N) from the beginning of the record until the mid-1970s and gradually decreased thereafter (Trenberth and Fasullo 2007). Within the last century, precipitation levels have increased by 7 to 10% in Switzerland and by 5 to 15% in France (Begert et al. 2005, Spagnoli et al. 2002). Zhang et al (2000). indicated that annual precipitation has increased in southern Canada by 5% to 35% since 1900.

Quebec, the region in North America that receives the second-highest amount of snowfall (between 200 and 300 cm per year on average) after the Rockies (Dorsaz and Brown 2008), is at risk of flooding because of the winter snowmelt that results in spring flooding (Assani and Tardif 2005, Larocque et al. 2010, Nastev et al. 2005). Additionally, Quebec produces the majority of its electricity through hydroelectric power. In fact, hydroelectricity represents nearly 97% of the electrical energy consumed in the region. However, few studies have been conducted on the spatial and temporal variability of precipitation since the 1970s in Quebec. Groleau et al. (2007) used the Mann Kendall test to analyze the spatiotemporal variability of rainfall data series from 1960-2005 for January and February. Yagouti et al. (2008) applied linear regression to analyze the spatiotemporal variability of snow amounts from January to March. Consequently, these studies analyzed precipitation variability only during short-term periods.

As a result of its dynamic properties, the atmosphere can accommodate an extensive range of temporal and spatial wave motions that may interact via complex nonlinear effects. With the aid of correlation analysis and dominance frequency detection, it is possible to determine the variability of precipitation data. Several authors have examined the interaction between climate indices and their associated hydro-climatological variables within this context. These climate oscillations carry the signals of variability in the atmospheric and oceanic circulation (Goly and Teegavarapu 2012, Rossi et al. 2011, Seierstad et al. 2016, Ouarda et al. 2014, Niranjan et al. 2016) and allow the quantification of the temporal evolution of a climate process for a particular region (Lee et al. 2013, Kumar et al. 2017, Ouarda et al. 2021). Zhang et al. (2010) showed a significant effect of El Niño Southern Oscillation (ENSO) and the Pacific Decadal Oscillation (PDO) on the maximum daily precipitation during winter in North America. Shabbar et al. (1997) demonstrated that ENSO events affect precipitation from British Columbia through the Prairies to the Great Lakes. Furthermore, there was a significant correlation between the North Atlantic Oscillation (NAO) index and the frequency of daily total precipitation extremes over Ontario and southern Quebec during fall and winter. Consequently, Hurrell (1995) demonstrated that the NAO and ENSO explain a significant portion of the observed climate variability in North America. Recently, a study by Cannon (2015) indicated that El Nino is likely responsible for the decrease in the probability of precipitation extremes over the Great Lakes region (Ohio River Valley) and Alaska. There is also a significant negative correlation between the PDO and the total winter precipitation in southern Quebec (Assani and Guerfi 2017). Thiombiano et al. (2017) and Thiombiano et al. (2018) demonstrated that the Arctic Oscillation (AO) and the Pacific North American pattern (PNA) have the most significant influence on the intensity and frequency of

precipitation extremes over southern Canada based on data analysis of extreme daily precipitation data.

The present study was designed to assess the trend in precipitation time series over southern Quebec using a modified version of the original Mann-Kendall (MK) test, which accounts for serial correlation. The Mann-Kendall trend test (Kendall and Stuart 1967, Mann 1945) is one of the most widely used tests to detect trends in hydrological and climatological time series (Zhang et al. 2001, Fiala et al. 2021). It is mainly beneficial to use a non-parametric test since it is more suitable for non-normally distributed and censored data, commonly encountered in hydro-meteorological time series (Yue et al. 2002, Khaliq^b et al. 2009, Khaliq^a et al. 2009).

The presence of sudden changes in precipitation time series was investigated using a Bayesian multiple change point detection procedure designed for the detection of change in the relationship between the response variable and explanatory variables. This procedure can be used when time is used as an explanatory variable to detect temporal changes in the time series. Since climate oscillations may affect the evolution of precipitation extremes, the second objective of the present study is to identify regional climate indices showing significant relationships with total and maximum annual precipitation in Southeastern Quebec using correlation analysis and to explore interactions across a time-frequency range between southern Quebec's precipitation and selected climate indices using wavelet analysis. Wavelet analysis has been widely used for the analysis of precipitation events and their teleconnection with global climate (Canchala et al. 2020, Hermida et al. 2015, Jiang et al. 2014, Tan et al. 2016), as well as seasonal and monthly precipitation patterns (Aguilar et al. 2005, Chandran et al. 2016, Fritier et al. 2012, Kim 2004, Pathak et al. 2016, Wang et al. 2017).

This paper is organised as follows: The study area and data description are presented in sections 2 and 3. The methods used in this study are outlined in Section 4. Results and discussions are presented in Section 5, and conclusions are presented in Section 6.

2. Study Area

The study area is the southern region of the province of Quebec, Canada. Ontario borders the province on the west, the United States and New Brunswick on the south, Hudson Bay, Nunavut, Ungava Bay to the north, and Labrador on the east. Quebec has a total area of approximately 1,668 million square kilometers. Its water area is 185,927 square kilometers.

2.1 Data Description

Two datasets are used in this study. The first dataset comprises different climate oscillation indices, which pertain to the average condition of the atmosphere across an extended period and changes in this condition over time. Data on daily precipitation are included in the second dataset.

2.1.1 Climate Oscillation Data

The process of climate oscillation is a cyclical process affecting global and regional climate patterns. Positive values are generally assigned to the warm phase of the climate index, while negative values are assigned to the cold phase. Every teleconnection index is based on a specific set of parameters or elements, known as climate elements, which describe only a particular aspect of a climate. Climate elements can be classified as atmospheric, such as air pressure, air temperature, precipitation, or solar radiation, and non-atmospheric, such as sea surface temperature and ice cover.

The current study examines some of the prominent global climate oscillations to determine their effects on total and maximum annual precipitation in Quebec's southern region and to use them as potential predictors. This oscillation has a different periodicity, allowing both short-term and long-

term interpretations of climate and precipitation variables for the region. A description of the data period and the data source of each climate index is provided in Table 1.

2.1.2 Daily Precipitation Data

This study used data from 25 meteorological stations located evenly throughout the southern part of Quebec. These stations cover the three homogeneous hydroclimate regions identified in southern Quebec (e.g., Assani et al. (2011)), namely the southeast hydroclimate region (SE), the southwest hydroclimate region (SW), and the eastern hydroclimate region (E). The southeast hydroclimate region (SE) is located on the St. Lawrence River's right bank (south shore), east hydroclimate region (E) is situated north of 47°N; and the southwest hydroclimate region (SW), mainly located on the north shore (left bank) of the river.

The following variables are calculated using daily data: total and maximum annual precipitation, total and maximum seasonal precipitation, and the maximum number of consecutive wet days per year. Here, we define consecutive wet days per year by the number of consecutive days each year or month when water is higher than 0.1 mm.

Figure.1 illustrates the geographical distribution of meteorological stations. The record period ranges from 30 to 37 years. Table. 2 identifies the stations used in this study, along with their ID, coordinates, and record period.

3. Methods

3.1 Mann–Kendall test

Mann-Kendall tests are used to analyze the trend of the data series. The null hypothesis (H_0) states that time series do not show a trend, while the alternative hypothesis (H_1) implies that there is a trend (up or down).

Assuming the sample time series is $x(t)$; $[t = 1, 2, \dots, m]$, the test statistic S is defined by:

$$S = \sum_{k=1}^{m-1} \sum_{l=k+1}^m \text{sign}(x_l - x_k) \quad \text{where} \quad \text{sign}(x_l - x_k) = \begin{cases} 1 & \text{if } x_k \prec x_l \\ 0 & \text{if } x_k = x_l \\ -1 & \text{if } x_k \succ x_l \end{cases} \quad (1)$$

Whenever m is large enough, the distribution of the S statistic is well approximated by a normal distribution with a zero mean and a variance as shown by equation (2).

$$\text{Var}(S) = \frac{m(m-1)(2m+5)}{18} \sum_{k=1}^m t_k(t_k - 1)(2t_k + 5) \quad (2)$$

m represents the number of tied values, while t_k represents the number of ties for the k th tied value.

Z_s , the standardized Mann-Kendall test statistic, is calculated as follows:

$$Z_s = \begin{cases} \frac{S - I}{\sqrt{\text{Var}(S)}} & \text{si } S \succ 0 \\ 0 & \text{si } S = 0 \\ \frac{S + I}{\sqrt{\text{Var}(S)}} & \text{si } S \prec 0 \end{cases} \quad (3)$$

A Z_s positive value indicates an increasing trend, whereas a negative value reflects a decreasing trend. Finally, the null hypothesis is rejected at a fixed significance level α , when the value of $|Z_s|$ exceeds $Z_{I-(\alpha/2)}$. In order to account for autocorrelation in the data, Hamed and Rao (1998) modified

the variance of the MK statistic S . In this paper, variance correction was applied to Z_s by taking into account the significant lag-1 serial correlation coefficients.

3.2 Bayesian multiple change point detection procedure

This study employs the Bayesian change point method proposed by Seidou and Ouarda (2007) to evaluate abrupt changes in mean or trend direction for several hydro-climatic variables. Due to its ability to deal with an unknown number of changes, this method displays the complete probability distribution of change dates. It represents a generalisation to the Bayesian multivariate linear regression procedure presented by Seidou et al. (2007). In this procedure, multiple change points in the relationship between explanatory variables and response variables are identified as well as their magnitudes and positions. In the absence of specified explanatory variables, the procedure detects changes in the time series of the response variable.

Based on n observations and d independent variables, the dependent variable is represented by k_j ($j = 1, \dots, n$), whereas L_{ij} ($i = 1, \dots, d$ and $j = 1, \dots, n$) indicates the j^{th} value of the i^{th} independent variable. The multiple linear regression can be expressed by:

$$k_j = \sum_{i=1}^d \beta_i l_{ij} + \zeta_j \quad (4)$$

3.3 Correlation analysis

The correlation coefficient describes the linear relationship between two variables, explaining how well they are related by providing the magnitude (intensity) and sign (direction) of the relationship between them. Although many methods can be used to investigate correlation, Pearson's correlation coefficient (PCC), which is one of the most commonly used, is evaluated here. The

Pearson correlation coefficient, symbolized by r , between two variables, a and b , is defined as the covariance of the two variables divided by the product of their standard deviations :

$$r = \frac{n \sum ab - (\sum a) \times \sum b}{\sqrt{n \sum a^2 - (\sum a)^2} \times \sqrt{n \sum b^2 - (\sum b)^2}} \quad (5)$$

In this equation, n denotes the total number of observations in each variable. As the coefficient of determination in linear regression, the r^2 indicates the amount to which a can explain the variance in b . The statistical significance of r is assessed by testing the null hypothesis $H_0: r = 0$ (there is no correlation) versus $H_1: r \neq 0$ (there is a correlation). Test statistic t_r is computed as follows:

$$t_r = r \sqrt{\frac{n - 2}{1 - r^2}} \quad (6)$$

3.4 Wavelet analysis

3.4.1 Continuous wavelet transform

The CWT was developed to overcome the limitations of the Fourier transform, which decomposes the signal (time series data) into a series of sinusoidal functions with varying frequencies, thereby allowing the localization of the signals only in frequency. On the other hand, CWT breaks the signal down into wavelets capable of decomposing the signal in time and frequency (scale) by shifting and stretching them. The Fourier transformation $X(f)$ of a time series $x(t)$, which reveals the information associated with the frequency content f , is given by:

$$X(f) = \int_{-\infty}^{+\infty} x(t) e^{-2\pi i ft} dt \quad (7)$$

Torrence and Compo (1998) defined CWT as the convolution of a given continuous signal $x(t)$ with the local basis function $\psi_{n,s}(\eta)$, which is the rescaled, translated, and normalized form of the mother wavelet $\psi_0(\eta)$:

$$W_n^x(p) = \int_{-\infty}^{+\infty} x(t) \Psi_{n,p}^* dt \quad \text{and} \quad \Psi_{n,p} = \frac{1}{\sqrt{p}} \Psi_0\left(\frac{t-n}{p}\right) \quad (8)$$

In the expression above, p is the scale parameter, n is the translation (time localization) parameter, ψ_0 is the mother wavelet, and the asterisk (*) represents the complex conjugate of the wavelet. In this study, the Morlet function was used as the mother wavelet. The Morlet provides the optimal balance between time and frequency localization for most natural aspect and adequately describes non-stationary signals such as hydro-climatological ones (Jevrejeva et al. 2003). It provides a phase angle relationship and captures the oscillatory nature since it is a complex function made up of a number of oscillation waves.

For a discrete observation (g_n , $n = 1, \dots, N$) with uniform time steps δ_t at a finite number of locations, CWT is computed as follows:

$$W_n^g(p) = \left(\frac{\delta_t}{p}\right)^{\frac{1}{2}} \sum_{n'=1}^N g_{n'} \Psi_0^* \frac{(n'-n)\delta_t}{p} \quad (9)$$

As the wavelet runs off the edge of the convolution process near the beginning and end of the time series, there is a wraparound effect in CWT. Thus, the time series is padded with zeros to reduce

the variance of the time series near the edge, resulting in the cone of influence (COI). The COI is defined as the area affected by the padding (edge effects). In light of the COI, only periods smaller than $\frac{N}{2\sqrt{2}}$ are considered significant (Grinsted et al. 2004, Torrence and Compo 1998).

3.4.2 Cross wavelet transform

In time-frequency space, cross wavelet transformation (XWT) shows regions in which the two time series exhibit high common power. Assuming that we have two time series, X and Y , with CWTs $W_n^{x(t)}$ and $W_n^{y(t)}$, respectively, their XWT $W_n^{XY(p)}$ corresponds to the complex wavelet transform of the first time series and its complex conjugate (Torrence and Compo, 1998):

$$W_n^{XY}(p) = W_n^X(p) W_n^{Y*}(p) \quad (10)$$

In the case of two time series with significant XWT signals, there is a possible teleconnection and thus plausible causation between them. The XWT provides confidence levels based on the square root of the product of two chi-squared distributions. Torrence and Compo (1998) provide a comprehensive discussion of cross wavelet analysis. Even though XWT is a powerful tool for studying relationships between two time series, it must be interpreted cautiously in light of the original time series. As XWT is not a normalized measure, significant power will be detected in cases of covarying power as well as in cases of extreme high values in one of the time series. However, even though the two time series covary, XWT may not identify this relationship if the individual CWT of the time series shows low power. Consequently, wavelet coherence is recommended for significance testing of the inter-relation between two time series, which addresses the problems associated with XWT (Maraun and Kurths 2004).

3.4.3 Wavelet coherence analysis

Wavelet transform coherence (WTC) identifies regions where two time series vary in the frequency space but do not have high common power in the time domain. Instead of measuring the common power of the two series using XWT, WTC measures the intensity of the covariance between them in time-frequency space (Jevrejeva et al., 2003). Torrence and Webster (1999) described how the WTC of two time series can be calculated as follows:

$$R_n^2 = \frac{|S(s^{-1} W_n^{XY}(s))|^2}{S(s^{-1} |W_n^X(s)|^2) S(s^{-1} |W_n^Y(s)|^2)} \quad (11)$$

In this case, S is a smoothing operator. Wavelet coherence, which encompasses 0 to 1 inclusive values, is analogous to the traditional correlation coefficient and may be viewed as a localized coefficient of correlation within a time-frequency domain. Both XWT and WTC for two data series provide complementary information. Wavelet coherence is especially useful when there is a low wavelet power but a high level of coherence between two time series. Our analysis is based on the statistical tests developed by Torrence and Compo (1998). A Monte-Carlo method is also employed to estimate the statistical significance at the 5% level, as presented by Grinsted et al. (2004). The degree of coherence as indicated by some patterns in different regions of the WTC plots are indicative of a correlation between the two signals.

4. Results and discussions

4.1 Trend analysis

The results of the modified MK test are presented in Table 3. In this table, the Z statistics are depicted for each precipitation variable at each station. At levels, 5% and 10%, statistically significant trends are identified with the indices a and b, respectively, over the corresponding Z values.

The Z statistics indicate that the majority of total annual series have increasing statistically significant trends. Some non significantly negative trends are also recorded in some annual series.

The trend in the total annual precipitation reveals a significant increase for stations located south of 47°N. However, for the stations located north of 47°N (East hydroclimatic region), none of the obtained trends are statistically significant.

The Z statistics indicate that most of the series have increasing trends regarding the maximum annual precipitation series. However, none of these trends are statistically significant except for two stations in the southwest hydroclimatic region and three others in the southeast region.

Seasonal trends are examined further by monthly grouping data into two seasons: the rain season between May and October and the snow season between November and April. Overall, the trend for total rain-period precipitation is increasing, especially in the southwest hydroclimatic region, where all the trends are significant at the level of 5%. In the east hydroclimatic region, the total liquid precipitation series also showed increasing trends. Nevertheless, none of these trends are statistically significant. A mixed trend of decreasing and increasing is evident in the total snow precipitation series. It is important to note that not all trends are significant. Most of the significant trends are increasing in the southeast hydroclimatic region. However, the most significant decrease in trends occurs in the southwest hydroclimatic region except for St Charles de Mandeville and Ste Anne de la Perade stations.

In maximum seasonal time series, a mixed set of trends is observed. Some trends are significant at the level of 5%-10%, while others are not. Maximum rainfall series at most stations show increasing trends. In contrast, the maximum snow precipitation series show decreasing trends for most stations except for the St Come-de-Linniere station, which showed a significant positive trend.

Multiple studies have addressed the statistically significant and spatially coherent trends in observational precipitation data across Canada (Dai et al. 1997, Groisman and Easterling 1994, Mekis and Hogg 1999, Vinnikov et al. 1990). Stone et al. (2000) found that southern areas of Canada exhibit seasonally increasing trends in total precipitation due to an increase in the intensity of events at all levels during the 20th century. As the century progresses, increases have been concentrated in heavy and intermediate events, with the enormous changes occurring in the Arctic. A significant part of the variability in precipitation intensity can be attributed to dominant modes of atmospheric variability.

4.2 Change point detection

The Bayesian multiple change point detection method was applied to the series of total annual precipitation as well as the maximum annual precipitation and the number of maximum consecutive wet days per year in order to identify any change points in considering the time series.

It is important to note that the data presented in Table. 4. developed from segments with at least six years of data, thereby avoiding change points too close to the edges of the series or for which there is not enough information to justify a conclusion. Bayesian techniques were also applied to segments with data spanning three, four and, five years, and the results were consistent with those for segments with six years of data.

For most of the total annual precipitation and the maximum number of consecutive wet days per year, three shifts are detected in three periods: 1965-1975, 1985-1995, and 2005-2015, whereas most of the maximum annual precipitation shifted only from 2005 to 2015. As natural variables are random, the exact date of change may not be as crucial as the existence of the change, the approximate year, and the general trends before and after the change. Depending on the random

component for the years surrounding the change, the exact date might be one or two years different from the detected one.

In the late 1960s and early 1970s, atmospheric circulation patterns in the North Atlantic changed, which seems to have been correlated with changes in precipitation patterns. Hurrell (1995) indicates that the NAO pattern reversed around the middle sixties, with strong positive NAO indices since 1980. It was generally a weak pressure gradient across the Atlantic during the 1960s, and many blocking events occurred due to which winter pressures were actually higher in the north than in the subtropics, which matches the shift observed in most total annual precipitation and consecutive wet days.

The shifts in precipitation series values over the period from 1985 to 1995 are caused by the changes in overall atmospheric circulation. Several phenomena characterize the climatology of 1985-1995 that exhibit substantial deviations from the mean state of the atmosphere over several months and seasons. In the first instance, following nearly continuous 15 years of positive-phase conditions in the North Atlantic, Eurasia, and northern Africa, the return to an intense negative phase in the atmospheric North Atlantic oscillation (NAO) during November 1995-February 1996 had significant effects on temperature and precipitation patterns in those regions. For example, Perreault et al. (1999) observed a shift in the average annual rainfall in eastern Canada (including southern Quebec) and the United States in 1999. The NAO also contributed to the significant decrease in winter temperatures across large portions of Siberia and northern Russia from the levels that prevailed during the 1980s.

The change in maximum precipitation during 2005-2010 may be related to the persistent negative phase of the North Atlantic Oscillation (NAO) that has occurred several times over North America. It is important to note that there were several cold weather events and unusual snow accumulations

in several Northern Hemisphere countries during the period December 2009-January 2010–February 2010 (hereafter winter 2010) (Cattiaux et al. 2010).

4.3 Correlation analysis

A correlation analysis was conducted between the studied climate patterns and the annual precipitation series on the one hand and the maximum precipitation series on the other hand. The aim is to identify climate indices that can predict future precipitation levels in southern Quebec. The AO and NAOJ indices showed the most significant influence on the variability of total annual precipitation, whereas maximum annual precipitation is strongly correlated with the TNA and NAOJ. Correlation analysis results are summarized in Figures. 2 and .3. The identification of the indices as dominant covariates is based on counting the number of stations which were significantly correlated with the precipitation variables.

A significant positive correlation is observed between total annual precipitation and the AO from July to September at approximately 72% of the southeast stations. The significant Pearson coefficient varies on average between 27% and 44%. In contrast to the southeast, only 50% of stations in the southwest display a significant positive correlation between the two variables, with significant values ranging from 24% to 36% during July to October. Across the east region, there is no significant correlation between the AO and the annual precipitation totals. In conclusion, the relationship between total annual precipitation amounts and annual AO exhibits an east-west pattern. That means that the Pearson coefficient increases as one moves from east to west.

Although the NAOj is a regional expression of the AO (Thompson and Wallace 1998), the NAOj pattern was also identified as a dominant one due to its strong correlation to the total annual precipitation compared to other climatic indices considered in this study.

NAOj demonstrates a significant correlation with both the total annual precipitation and the maximum annual precipitation. The strongest correlation between the two variables is observed in the southeast region, where 57% of stations demonstrate a significant negative correlation between NAOj and total annual precipitation between April and July for most stations. Only a few stations are correlated with NAOj from August to November. Approximately half of the stations in the southwest region show a relationship between NAOj and total annual precipitation between April and July. The same percentage is found in the east region, where the relationship between the variables is negatively significant between September and December. The significant Pearson coefficient varies on average between 24% and 39%.

Furthermore, the relationship between the NAOj and the maximum annual precipitation is also quite strong in the southeast. In this region, the coefficients have a negative range between 26% and 39% between April and July, where the correlation is most prominent. On the other hand, no dominant period is prominent in the southwest region, although there is a negative correlation between maximum annual precipitation and the NAOj. In the eastern region, the correlation between these two variables is negative, significant between March and July.

The TNA index has also influenced maximum annual precipitation in the southern part of the province of Quebec. Indeed, there is a strong positive correlation between both variables. This dependence is most pronounced in the southeast region, and its significance is observed between August and October. The dependence also tends to increase from east to west.

4.5 Wavelet analysis

The AO, NAOj, and TNA climate indices were the most significant regional dominant patterns based on correlation analysis. Due to space limitations, wavelet analysis results are only displayed at three node stations: LINGWICK (Southeast Regional), ST CHARLES DE MANDEVILLE

(Southwest Regional), and ST JEAN DE CHERBOURG (East Regional) with the monthly average window of each climate index value during the period of significant correlation.

4.5.1 Continuous Wavelet Transform: CWT

In order to determine the dominant frequency of annual precipitation and maximum precipitation, wavelet transforms were conducted. The CWT graphs for both variable series are depicted in Figures 4. and 5. A thick black contour in Figures and represents the 5% significance level against the red noise, whereas a lighter shade represents the cone of influence where edge effects might distort the picture.

The assessment of the CWTs of the total annual precipitation analyzed time series revealed significant variability principally in the range of periods from 1 to 3 years in the southeast and southwest regions. Nonetheless, these shorter cycles are irregularly distributed along the period of record. In these locations, the larger identified cycles have approximately two years, beginning in the decade of 1980, as is shown in Figures 4. (a) and 4. (b). In the eastern region, total annual precipitation reveals a more robust and more extensive cycle. In the St. Jean de Cherbourg station, three primary cycles can be observed, as shown in the Figure 4 (c). the period lasted for 1-3 years, 6-8 years, and 12-14 years, respectively, beginning in 1980 and ending in 1990, 1985, and 1992.

Maximum annual precipitation series exhibit 8- to 4-year cycles continuously possessing significant powers during the periods of 1975–1990 in the southeast and eastern region and 1985–2005 in the southwest region.

Figure 5. illustrates the results obtained from WTCs results at each of the three stations. In addition to the cycles mentioned, CHARLES DE MANDEVILLE exhibits a decisive 2-3 year cycle between 1990 and 1995.

In order to investigate the influence of large-scale climate indices on precipitation in southern Quebec, the continuous wavelet transform was also applied to dominate the frequency domain of selected teleconnection indices. The results are depicted in Figure. 6.

The AO average values for JFM mean values time series continuous wavelet analysis, which is shown in Figure. 6 (a), for the period from 1951 to 2018, revealed a short cycle spanning 1-2 years during 1998-2003 and a second cycle spanning about 3-4 years from 2010 to 2015. This concords with the WTC result of CHARLES DE MANDEVILLE station and confirms the correlation analysis results where the most significant pearson coefficient is observed between the total annual precipitation time series recorded at this station and the average mean values of the AO index over this period.

The strongest correlation was found between the total annual precipitation time series in the eastern region and the AO index during the period April May June. For exemple, during this period, at the St. Jean Charlbourg station, WTC analysis of the AO index reveals two significant periodicities, the first occurring between 1987 and 2005 at an 8-14 year scale and the second occurring between 1990 and 1995 at a four-year scale. These coincide with the periodicity of the time series examined at this station.

During July and September, the AO time series exhibits two prominent periodicities of 2-3 years and 6-8 years over 1980-1990 and 1990-1995, respectively. Despite the strongest pearson coefficient of the correlation analysis being found at this period at LINGWICK Station, there is no coincidence in the periodicity of those two variables.

From April to July, the NAOj time series exhibits a strong periodicity of 14-16 years period 1990-2005. Other significant periodicities are also detected in August-September and October at a scale of 1-2 years between 2010 and 2015 and 6-8 years between 1985 and 1995. There is a significant

agreement between the period of records for significant cycles between the NAOj index and the total and maximum annual precipitation series at the chosen stations.

The TNA index exhibits a periodicity within the range of 8-10 during the strongest correlation period. A periodicity within the 2-4 years band is also detected. Significant periodicities are found to exist between TNA and the total and maximum annual precipitation time series.

4.5.2 Cross-wavelet transform: XWT

The XWT plot between total and maximum annual precipitation amounts and the AO index allows highlighting that the common features from the individual CWT are significant at the 5 % level, given that significant common power is observed in the 2–4-year band around 1990 and 1980 at LINGWICK station (Figure 7. (a)), around 2000 and 2010 at ST CHARLES DE MANDEVILLE station (Figure 7. (b)) and around 1970 at ST JEAN DE CHERBOURG (Figure 7. (c)).

A notable persisting common power is observed in the 14–16-year band around 1980 and 2005 at ST JEAN DE CHERBOURG. It is expected that cause-and-effect relations between the phenomena recorded in the time series will exist when the oscillations are phase locked. It is thus comforting to see that the XWT graph reveals that precipitation and AO are in phase in all sectors with high significant common power, confirming a strong connection between AO and precipitation.

The NAOj and total annual precipitation XWT plot (Figure. 7 (d, e and f), shows a slightly noticeable significant region around 2010 at LINGWICK, around 1990-2005 at ST CHARLES DE MANDEVILLE and around 1970-1990 at ST JEAN DE CHERBOURG with a 2-3 years' period. A notable persisting common power is observed in the 14–16-year band around 1980 and 2005 at ST JEAN DE CHERBOURG. When looking at the maximum annual precipitation plotted against the NAOj XWT (Figure 8. (a, b and c), two- to three-year periods are observed at all three

stations around 1985, 1990, and 1970. Except for ST JEAN DE CHERBOURG, significant common power can also be detected in the 6-8-year band between 1980 and 1990.

There is a slight correlation between TNA and the maximum annual precipitation at LINGWICK (Figure 8. (d)) station between 1970 and 1990, as well as between 1990 and 2000 between ST CHARLES DE MANDEVILLE Figure 8. (e)). Several similar characteristics were detected at the same station during the same period but on a scale of six to eight years.

Strong power is detected in ST JEAN DE CHERBOURG Figure 8. (f)) on the scale of 8-10 years between 1975 and 2000.

Finally, XWT and WTC results indicate that these data sets are in phase, supporting the correlation between the teleconnections index and the variables of interest.

4.5.3 Wavelet transform coherence

4.5.3.1 Arctic oscillation : AO

WTCs between total annual precipitation times series of the three mentioned stations and AO (NAOj) climate index are shown in Figures 9. (a, b and c). According to a Monte Carlo experiment, black contours indicate periods of statistically significant coherence in the thick red noise process at a 5% significance level (Grinsted et al. 2004, Jevrejeva et al. 2003).

Overall, the total annual precipitation and the AO index of the three stations show significant coherence at time scales and distinct periods. As shown in Figure 9. (a), the AO index strongly coincides with the total annual precipitation in LINGWICK during July–August–September in the period of 12–16 years from 1975 till 2005. It is a long lasting pattern. Both signals are in phase, which indicates a positive correlation. This confirms the results of the correlation analysis.

LINGWICK also exhibits significant coherence during July, August, and September of the 6–8 year period of 1980–2000. Significant coherence was also detected at the 2–4 year level between 1970–1975 and 1990–1995. AO exhibits positive coherence at ST CHARLES DE MANDVILLE and during January–February–Mars from 1980–1995 with periods 17 to 18 years long. An in-phase relationship is clearly indicated by the arrows pointing to the right (Figure 9. (b)). For ST JEAN DE CHERBOURG, AO exhibits a strong positive coherence between April–May–June on the scale of 2–4 years and 6–8 years from 1970 to 1990 and 2000–2005, respectively. A positive correlation is also detected with a 14–16 year period from 1990–2000 (Figure 9. (c)).

These results provide elements that may be included in a more accurate precipitation prediction for these regions. For example, Assani et al. (2008) found that precipitation correlates positively with the AO index in the Saint-François River watershed. There were multiple warm and moist air masses in the Gulf of St. Lawrence and Bay of Fundy, and it appears that their frequency increased with the positive values of the AO index, leading to more precipitation.

4.5.3.2 North Atlantic Oscillation (Jones) : NAOj

NAOj is the second dominant climate pattern that impacts both total annual precipitation and maximum annual precipitation. The corresponding WTCs between Max annual precipitation time series at the three stations and the NAOj climate index are computed. The results are presented in Figures 10 and 11. Globally, the total annual precipitation, maximum annual precipitation, and NAOj index show significant negative coherence across time scales and periods. From April–May–June in 1988–1992, there is a strong negative correlation between the total annual precipitation and the NAOj at the LINGWICK station. By the pointing left arrows, the antiphase is obvious.

A persisting coherence is detected in the 8–12 years band. NAOj appears to be ahead of annual precipitation at this station, as indicated by up arrows. Also, significant negative coherence is

detected between NAOj and maximum annual time series at this station for May-June-July over 2-3 years and 1-2 years between 1965-1972 and 1985-1987, respectively.

When evaluating the total annual precipitation at ST CHARLES DE MANDEVILLE station, NAOj exhibits negative coherence during April-May-June from 1960-1965, with periods of 2 to 4 years. By pointing to the left, the arrows present a clear indication of an antiphase relationship. A strong negative coherence is detected between 1985 and 1995 for the 6-8-year band. Additionally, a strong persisting coherence is found between 1980 and 2005 between the 8-12 year bands. The strongest association between NAOj and maximum annual precipitation was observed during the same period of total annual precipitation but at a scale of 1-3 years from 1990 to 2000. Coherence is negative, which supports the result of the correlation analysis.

ST JEAN DE CHERBOURG's annual precipitation times series display a negative correlation with NAOj. Interestingly, as illustrated in figure 10. (c), there was a very strong correlation between the NAOj and the total annual precipitation during the period of May-June-July over a period of 2-3 years, around 1970, 1990 and 2010. The maximum annual precipitation and NAOj also show a strong negative correlation over a three quarters period from 2000 to 2010, particularly during August-September-October. Around 1980, a tiny coherence of 10-12 years was also detected.

The statistically significant correlation between climate indexes and precipitation time series, as observed in many studies as well as in the present study, is attributable to physical processes associated with the flux dynamics of air masses throughout the world. For instance, Thompson and Wallace (2001) described the relationship between sea level pressure variability, wind direction, and warm-cool phases of the AO, NAO, and PNA. Wu et al. (2005) reported as well that anomalous northerlies from the Arctic region sent colder air to northeastern Canada, generating negative temperature anomalies there. Over eastern Canada, the North Atlantic

oscillation (NAO) is the most crucial mode of atmospheric variability. The Icelandic Low is usually deep in positive NAO years, resulting in cold Arctic air moving southward to the area west of Iceland and Greenland, causing cold anomalies over eastern Canada (Hurrel 1995). According to Whan et al. (2016), NAO influence on extreme precipitation is strongest in eastern North America, with the likelihood of negative phase extreme rainfall events decreasing in the north and increasing in the south under the positive phase of the NAO. We feature our results since NAOj is a regional expression of NAO.

4.5.3.3 Tropical Northern Atlantic oscillation: TNA

According to the results of the correlation analysis, the tropical north Atlantic index is the second persistent index that influences the maximum annual precipitation time series.

Coherence results of the wavelet transform for selected stations confirm the correlation analysis (Figure 12. (a, b and c)). The LINGWICK station, for example, shows a strong correlation between the indices between 1994 and 1997 and a persisting positive correlation at the scale of 7-9 years between 1997 and 2005.

At ST CHARLES DE MANDEVILLE the strongest coherence was found between 1985-2010 within the 7-10-year band. ST JEAN DE CHERBOURG station exhibits the strongest correlation between TNA and maximum annual precipitation data.

Positive coherences persist from 1985 to 2010 at a time scale of eight to ten years.

Furthermore, it is essential to note that the tropical North Atlantic region is strongly affected by both the NAO and ENSO phenomena. The significance of this result lies in the fact that it was never suggested that the TNA could affect extreme precipitation in this region.

5. Conclusions and future works

With a long-term precipitation trend analysis of 25 total precipitation time series in southern Quebec, this study allows to conclude that a majority of precipitation stations show significant increasing trends over the recent years. As a result of the trend analysis in total annual precipitation, stations located south of 47°N indicate the most significant increasing trends. On the other hand, none of the obtained trends are statistically significant for the stations north of 47°N. Seasonal trend analysis indicates that a wide range of precipitation stations show significant increases during the rainy season. However, quite a few of these showed an increase in snow seasons.

In the following investigation, we examined the abrupt changes in annual precipitation behavior. The Bayesian multiple change-point detection procedure also supported the increasing trend in total annual precipitation. Most change points were observed between 1965-1985 and 1985-1995 for the total annual precipitation and between 2005-2015 for the maximum annual precipitation.

Correlation analysis and wavelet analysis were conducted on the preceding three-monthly moving average values of the different climate patterns and annual precipitation values. The results of this investigation allowed us to retain three dominant climate patterns within the study area, namely the AO, NAOj, and TNA indices. The total annual precipitation positively correlates with the AO and negatively with the NAOj. The analysis shows also that maximum annual precipitation is in phase with the TNA index and in opposite phase with the NAOj index.

Precipitation totals on an annual scale are subject to significant cycles lasting two to three years. In contrast with the east region, the periodicity in the southeast and southwest regions is relatively weak. In terms of annual precipitation, a 2- to 3-year cycle is marked. Meanwhile, maximum annual precipitation shows 4- to 8- year significant cycles.

The XWT plots revealed that the relationship between the total and maximum precipitation data and the retained climate indices in the eastern region is more significant when compared to those of the southeastern and southwest regions. The WTC plots demonstrate a high degree of coherence between the retained indices and the variables of the interests.

Finally, teleconnection patterns are among the most reliable covariates in precipitation prediction models due to their predictable nature and significant influence. According to our findings, the AO, NAOj, and TNA patterns can be used as predictors for the long-term prediction of total and maximum annual precipitation in southern Quebec.

References

- Aguilar, E., Peterson, T., Obando, P.R., Frutos, R., Retana, J.A., Solera, M., Soley, J., García, I.G., Araujo, R. and Santos, A.R. (2005) Changes in precipitation and temperature extremes in Central America and northern South America, 1961–2003. *Journal of Geophysical Research: Atmospheres* 110(D23).
- Assani, A., Lajoie, F., Vadnais, M. and Beauchamp, G. (2008) Influence of the Arctic oscillation on the internannual variability of precipitation in the Saint-François river watershed (Québec, Canada) as determined by canonical correlation analysis. *Revue des sciences de l'eau* 21(1).
- Assani, A. and Tardif, S. (2005) Classification, caractérisation et facteurs de variabilité spatiale des régimes hydrologiques naturels au Québec (Canada). Approche éco-géographique. *Revue des sciences de l'eau/Journal of Water Science* 18(2), 247-266.
- Assani, A.A., Chalifour, A., Légaré, G., Manouane, C.-S. and Leroux, D. (2011) Temporal regionalization of 7-day low flows in the St. Lawrence watershed in Quebec (Canada). *Water resources management* 25(14), 3559-3574.
- Assani, A.A. and Guerfi, N. (2017) Analysis of the Joint Link between Extreme Temperatures, Precipitation and Climate Indices in Winter in the Three Hydroclimate Regions of Southern Quebec. *Atmosphere* 8(4), 75.
- Barbulescu, A. (2016) A new method for estimation the regional precipitation. *Water resources management* 30(1), 33-42.
- Begert, M., Schlegel, T. and Kirchhofer, W. (2005) Homogeneous temperature and precipitation series of Switzerland from 1864 to 2000. *International Journal of Climatology: A Journal of the Royal Meteorological Society* 25(1), 65-80.
- Canchala, T., Alfonso-Morales, W., Cerón, W.L., Carvajal-Escobar, Y. and Caicedo-Bravo, E. (2020) Teleconnections between monthly rainfall variability and large-scale climate indices in southwestern Colombia. *Water* 12(7), 1863.
- Cannon, A.J. (2015) Revisiting the nonlinear relationship between ENSO and winter extreme station precipitation in North America. *International Journal of Climatology* 35(13), 4001-4014.

Chandran, A., Basha, G. and Ouarda, T. (2016) Influence of climate oscillations on temperature and precipitation over the United Arab Emirates. *International Journal of Climatology* 36(1), 225-235.

Cattiaux, J., Vautard, R., Cassou, C., Yiou, P., Masson-Delmotte, V., & Codron, F. (2010). Winter 2010 in Europe: A cold extreme in a warming climate. *Geophysical Research Letters*, 37(20).

Dai, A., Fung, I.Y. and Del Genio, A.D. (1997) Surface observed global land precipitation variations during 1900–88. *Journal of Climate* 10(11), 2943-2962.

Dorsaz, F. and Brown, R. (2008) Évaluation des simulations du couvert nival sur le Québec par les modèles MRCC 4.2. 3 et GEMCLIM 3.3. 0. Rapport de stage, Ouranos 49.

Ehsanzadeh, E. and Adamowski, K. (2010) Trends in timing of low stream flows in Canada: Impact of autocorrelation and long-term persistence. *Hydrological Processes: An International Journal* 24(8), 970-980.

Fiala, T., Ouarda, T.B.M.J., and J. Hladny (2010). Evolution of low flows in the Czech Republic, *Journal of Hydrology*, 393 (2010) 206–218.

Fritier, N., Massei, N., Laignel, B., Durand, A., Dieppois, B. and Deloffre, J. (2012) Links between NAO fluctuations and inter-annual variability of winter-months precipitation in the Seine River watershed (north-western France). *Comptes Rendus Géoscience* 344(8), 396-405.

Goly, A. and Teegavarapu, R.S. (2012) Influence of teleconnections on spatial and temporal variability of extreme precipitation events in Florida, pp. 1899-1908.

Grinsted, A., Moore, J.C. and Jevrejeva, S. (2004) Application of the cross wavelet transform and wavelet coherence to geophysical time series. *Nonlinear processes in geophysics* 11(5/6), 561-566.

Groisman, P.Y. and Easterling, D.R. (1994) Variability and trends of total precipitation and snowfall over the United States and Canada. *Journal of Climate* 7(1), 184-205.

Groleau, A., Mailhot, A. and Talbot, G. (2007) Trend analysis of winter rainfall over southern Québec and New Brunswick (Canada). *Atmosphere-Ocean* 45(3), 153-162.

Hermida, L., López, L., Merino, A., Berthet, C., García-Ortega, E., Sánchez, J.L. and Dessens, J. (2015) Hailfall in southwest France: Relationship with precipitation, trends and wavelet analysis. *Atmospheric Research* 156, 174-188.

Hurrell, J.W. (1995) Decadal trends in the North Atlantic Oscillation: Regional temperatures and precipitation. *Science* 269(5224), 676-679.

IPCC (2012) Managing the risk of extreme events and disasters to advance climate change adaptation. Special Report of the Intergovernmental Panel on Climate Change (IPCC). A special report of working groups I, II of the IPCC. Cambridge University Press, Cambridge, UK, and New York, NY, USA.

Jevrejeva, S., Moore, J. and Grinsted, A. (2003) Influence of the Arctic Oscillation and El Niño-Southern Oscillation (ENSO) on ice conditions in the Baltic Sea: The wavelet approach. *Journal of Geophysical Research: Atmospheres* 108(D21).

Jiang, R., Gan, T.Y., Xie, J. and Wang, N. (2014) Spatiotemporal variability of Alberta's seasonal precipitation, their teleconnection with large-scale climate anomalies and sea surface temperature. *International Journal of Climatology* 34(9), 2899-2917.

Kendall, M.G. and Stuart, A. (1967) The Advanced Theory of Statistics. Population (18^e année), 396-396.

Khaliq, M.N., Ouarda, T.B.M.J., Gachon, P., SUSHAMA, L., and A. ST-HILAIRE (2009). Identification of hydrological trends in the presence of serial and cross correlations: A review of selected methods and their application to annual flow regimes of Canadian rivers, *Journal of Hydrology*, 368: 117-130

Khaliq, M.N., Ouarda, T.B.M.J., and P. Gachon (2009). Identification of temporal trends in annual and seasonal low flows occurring in Canadian rivers: The effect of short- and long-term persistence, *Journal of Hydrology*. doi:10.1016/j.jhydrol.2009.02.045, 368: 183-197

Kim, S. (2004) Wavelet analysis of precipitation variability in northern California, USA. *KSCE Journal of Civil Engineering* 8(4), 471-477.

Kumar, K.N., Molini, A., Ouarda, T.B.M.J. and Rajeevan, M.N. (2017). North Atlantic controls on wintertime warm extremes and aridification trends in the Middle East, *Scientific Reports*, 7(1): 12301.

Larocque, M., Fortin, V., Pharand, M. and Rivard, C. (2010) Groundwater contribution to river flows—using hydrograph separation, hydrological and hydrogeological models in a southern Quebec aquifer. *Hydrology and Earth System Sciences Discussions* 7(5), 7809-7838.

Lee, T., Ouarda, T.B.M.J. and Li, J. (2013) An orchestrated climate song from the Pacific and Atlantic Oceans and its implication on climatological processes. *International Journal of Climatology* 33(4), 1015-1020.

Mann, H.B. (1945) Nonparametric tests against trend. *Econometrica: Journal of the econometric society*, 245-259.

Maraun, D. and Kurths, J. (2004) Cross wavelet analysis: significance testing and pitfalls. *Nonlinear processes in geophysics* 11(4), 505-514.

Mekis, E. and Hogg, W.D. (1999) Rehabilitation and analysis of Canadian daily precipitation time series. *Atmosphere-Ocean* 37(1), 53-85.

Moazenzadeh, R., Mohammadi, B., Shamshirband, S. and Chau, K.-w. (2018) Coupling a firefly algorithm with support vector regression to predict evaporation in northern Iran. *Engineering Applications of Computational Fluid Mechanics* 12(1), 584-597.

Nastev, M., Rivera, A., Lefebvre, R., Martel, R. and Savard, M. (2005) Numerical simulation of groundwater flow in regional rock aquifers, southwestern Quebec, Canada. *Hydrogeology journal* 13(5), 835-848.

Ouarda, T.B.M.J., Charron, C., Mahdi, S. and Youssef, L.A. (2021). Climate teleconnections, interannual variability, and evolution of the rainfall regime in a tropical Caribbean island: case study of Barbados, *Theoretical and Applied Climatology*.

Ouarda, T.B.M.J., Charron, C., Niranjan Kumar, K., Marpu, P., Ghedira, H., Molini, A., Khayal, I. (2014). Evolution of rainfall regime in the UAE, *Journal of Hydrology*, 514 (June): 258–270.

Pathak, P., Kalra, A., Ahmad, S. and Bernardez, M. (2016) Wavelet-aided analysis to estimate seasonal variability and dominant periodicities in temperature, precipitation, and streamflow in the Midwestern United States. *Water resources management* 30(13), 4649-4665.

Rossi, A., Massei, N. and Laignel, B. (2011) A synthesis of the time-scale variability of commonly used climate indices using continuous wavelet transform. *Global and Planetary Change* 78(1-2), 1-13.

Seidou, O. and Ouarda, T.B.M.J (2007) Recursion-based multiple changepoint detection in multiple linear regression and application to river streamflows. *Water Resources Research* 43(7).

Seidou, O., Asselin, J.J., and T.B.M.J., Ouarda (2007). Bayesian multivariate linear regression with application to changepoint models in hydrometeorological variables, *Water Resources Research*. 43, W08401.

Seierstad, I.A., Stephenson, D.B. and Kvamstø, N.G. (2016) How useful are teleconnection patterns for explaining variability in extratropical storminess? *Tellus A: Dynamic Meteorology and Oceanography* 59(2), 170-181.

Shabani, S., Samadianfard, S., Sattari, M.T., Mosavi, A., Shamshirband, S., Kmet, T. and Várkonyi-Kóczy, A.R. (2020) Modeling pan evaporation using gaussian process regression k-nearest neighbors random forest and support vector machines; Comparative analysis. *Atmosphere* 11(1), 66.

Shabbar, A., Bonsal, B. and Khandekar, M. (1997) Canadian precipitation patterns associated with the Southern Oscillation. *Journal of Climate* 10(12), 3016-3027.

Spagnoli, B., Planton, S., Déqué, M., Mestre, O. and Moisselin, J.M. (2002) Detecting climate change at a regional scale: the case of France. *Geophysical Research Letters* 29(10), 90-91-90-94.

Stone, D.A., Weaver, A.J. and Zwiers, F.W. (2000) Trends in Canadian precipitation intensity. *Atmosphere-Ocean* 38(2), 321-347.

Tan, X., Gan, T.Y. and Shao, D. (2016) Wavelet analysis of precipitation extremes over Canadian ecoregions and teleconnections to large-scale climate anomalies. *Journal of Geophysical Research: Atmospheres* 121(24), 14,469-14,486.

Thiombiano, A.N., El Adlouni, S., St-Hilaire, A., Ouarda, T.B.M.J. and El-Jabi, N. (2017). Nonstationary frequency analysis of extreme daily precipitation amounts in Southeastern Canada using a peaks-over-threshold approach, *Theoretical and Applied Climatology*, 129(1-2): 413-426. doi:10.1007/s00704-016-1789-7.

Thiombiano, A.N., St-Hilaire, A., El Adlouni, S.-E. and Ouarda, T.B.M.J. (2018) Nonlinear response of precipitation to climate indices using a non-stationary Poisson-generalized Pareto model: case study of southeastern Canada. *International Journal of Climatology* 38, e875-e888.

Torrence, C. and Compo, G.P. (1998) A practical guide to wavelet analysis. *Bulletin of the American Meteorological Society* 79(1), 61-78.

Torrence, C. and Webster, P.J. (1999) Interdecadal Changes in the ENSO–Monsoon System. *Journal of Climate* 12, 2679-2690.

Trenberth, K.E. and Fasullo, J. (2007) Water and energy budgets of hurricanes and implications for climate change. *Journal of Geophysical Research: Atmospheres* 112(D23).

Vinnikov, K.Y., Groisman, P.Y. and Lugina, K. (1990) Empirical data on contemporary global climate changes (temperature and precipitation). *Journal of Climate* 3(6), 662-677.

Wang, B., Li, J. and He, Q. (2017) Variable and robust East Asian monsoon rainfall response to El Niño over the past 60 years (1957–2016). *Advances in Atmospheric Sciences* 34(10), 1235-1248.

Whan, K., Zwiers, F. and Sillmann, J. (2016) The influence of atmospheric blocking on extreme winter minimum temperatures in North America. *Journal of Climate* 29(12), 4361-4381.

Wu, A., Hsieh, W.W. and Shabbar, A. (2005) The nonlinear patterns of North American winter temperature and precipitation associated with ENSO. *Journal of Climate* 18(11), 1736-1752.

Yagouti, A., Boulet, G., Vincent, L., Vescovi, L. and Mekis, É. (2008) Observed changes in daily temperature and precipitation indices for southern Québec, 1960–2005. *Atmosphere-Ocean* 46(2), 243-256.

Yue, S., Pilon, P. and Cavadias, G. (2002) Power of the Mann–Kendall and Spearman's rho tests for detecting monotonic trends in hydrological series. *Journal of Hydrology* 259(1-4), 254-271.

Zhang, X., Harvey, K.D., Hogg, W. and Yuzyk, T.R. (2001) Trends in Canadian streamflow. *Water Resources Research* 37(4), 987-998.

Zhang, X., Wang, J., Zwiers, F.W. and Groisman, P.Y. (2010) The influence of large-scale climate variability on winter maximum daily precipitation over North America. *Journal of Climate* 23(11), 2902-2915.

LIST OF TABLES

TABLE 1. CLIMATE OSCILLATION INDICES CONSIDERED IN THE STUDY	52
TABLE 2. CHARACTERISTICS OF THE CLIMATIC STATIONS USED IN THE STUDY.	53
TABLE 3. RESULTS OF THE MODIFIED MK TEST FOR ANNUAL AND SEASONAL PRECIPITATION TIME SERIES.....	56
TABLE 4. YEARS OF CHANGE FOR TOTAL ANNUAL PRECIPITATION (V1), MAXIMUM ANNUAL PRECIPITATION (V2) AND MAXIMUM CONSECUTIVE WET DAYS (V3).....	59

Table 1. Climate Oscillation Indices considered in the study

Climate Oscillation Indices	Short name	Recording Period
El Niño Southern Oscillation	ENSO	1951 – 2019
The Pacific North American pattern	PNA	1951 – 2019
Pacific Decadal Oscillation	PDO	1951 – 2019
North Atlantic Oscillation	NAO	1951 – 2019
North Atlantic Oscillation (Jones)	NAOJ	1951 – 2019
Atlantic Multidecadal Oscillation	AMO	1951 – 2019
Tropical Northern Atlantic Index	TNA	1951 – 2019
Eastern Atlantic index	EA	1951 – 2019
Western Hemisphere warm pool	WHWP	1951 – 2019
Arctic Oscillation	AO	1951 – 2019
Southern Oscillation Index	SOI	1951 – 2019
Oceanic Niño Index	ONI	1951 – 2019

Table 2. Characteristics of the climatic stations used in the study.

Code	Station	ID	Altitude (m)	Latitude (N)	Longitude (W)	Years
SE1 (1)	ST ANICET	7026836	53.30	45.13	-74.35	60
SE2 (2)	ORMSTOWN	7025745	45.70	45.12	-74.05	57
SE3 (3)	HEMMINGFORD FOUR WINDS	7023075	61	45.07	-73.72	60
SE4 (4)	GRANBY	7022800	175	45.38	-72.72	72
SE5 (5)	COATICOOK	7021840	259.10	45.15	-71.8	71
SE6 (6)	ST MALO D'AUCKLAND	7027520	564.00	45.2	-71.5	57
SE7 (7)	LINGWICK	7024320	266.70	45.63	-71.37	68
SE8 (8)	ST LUDGER	7027516	335.00	45.75	-70.68	56
SE9 (9)	ST COME DE LINIERE	7027083	243.8	46.05	-70.52	55
SE10 (10)	ST CAMILLE	7056930	396.00	46.48	-70.22	57

SE11	SCOTT	7027840	144.8	46.5	-71.08	52
(11)						
E1	ST AMBROISE	7066820	121.90	48.57	-71.33	66
(12)						
E2	BAGOTVILLE A	7060400	159.10	48.33	-71	78
(13)						
E3	LAC HUMQUI	7053649	235.9	48.28	-67.57	49
(14)						
E4	MONT JOLI A	7055121	52.4	48.61	-68.21	78
(15)						
E5	ST JEAN DE	7057395	350.5	48.88	-67.12	58
(16)	CHERBOURG					
E6	CAP DES ROSIERS	7051055	15	48.85	-64.2	47
(17)						
SW1	WRIGHT	7038975	141,70	46.07	-76.05	53
(18)						
SW2	ANGERS	7030170	91	45.55	-75.55	58
(19)						
SW3	LACHUTE	7033650	91.40	45.65	-74.33	57
(20)						
SW4	COTEAU DU LAC	7011947	49.40	45.32	-74.17	54

(21)

SW5	ST CHARLES DE	7016960	167.60	46.35	-73.35	99
(22)	MANDEVILLE					
SW6	ST ALBAN	7016800	76.20	46.72	-72.08	71
(23)						
SW7	LAC AUX SABLES	701LEEH	160	46.87	-72.4	56
(24)						
SW8	STE ANNE DE LA	7016840	16	46.58	-72.23	71
(25)	PERADE					

Table 3. Results of the modified MK test for annual and seasonal precipitation time series.

code	Station	Variables					
		Annual total precipitation	Annual max precipitation	Total liquid precipitation	Max liquid precipitation	Total solid precipitation	Max solid precipitation
SE1 (1)	ST ANICET	3.39 ^a	1.45	2.65 ^a	1.65 ^b	-0.27	0.29
SE2 (2)	ORMSTOWN	2.66 ^a	1.73	3.07 ^a	1.70 ^b	0.66	0.23
SE3 (3)	HEMMINGFORD	2.88 ^a	2.76 ^a	2.26 ^a	2.04 ^a	1.15	-0.31
	FOUR WINDS						
SE4 (4)	NICOLET	-2.72 ^a	-2.31 ^a	-0.36	-2.11 ^a	-3.68 ^a	-3.50 ^a
SE5 (5)	GRANBY	2.73 ^a	0.31	2.98 ^a	-0.11	0.76	0.69
SE6 (6)	COATICOOK	4.83 ^a	1.57	4.64 ^a	0.85	1.10	0.51
SE7 (7)	ST MALO	-0.14	0.74	2.33 ^a	0.90	0.45	0.31
	D'AUCKLAND						
SE8 (8)	LINGWICK	4.32 ^a	1.26	2.45 ^a	1.16	4.25 ^a	1.46
SE9 (9)	ST LUDGER	0.72	2.79 ^a	2.05 ^a	2.35 ^a	0.00	-0.24
SE10 (10)	ST COME DE LINIERE	0.82	0.65	1.56	-0.45	-0.51	1.16 ^b

SE11 (11)	ST CAMILLE	3.82 ^a	1.64	3.75 ^a	1.83 ^b	2.90 ^a	1.01
SE12 (12)	SCOTT	1.85 ^b	0.54	2.36 ^a	-1.19	2.67 ^a	0.30
E1 (13)	ST AMBROISE	0.39	0.36	0.65	0.87	-0.25	-0.88
E2 (14)	BAGOTVILLE A	-0.11	0.74	0.50	1.04	1.89 ^b	-1.12
E3 (15)	LAC_HUMQUI	1.129	1.13	1.02	0.03	0.68	1.35
E4 (16)	Mont Joli A	0.480	0.48	1.24	0.71	-1.44	-1.56
E5 (17)	CAP DES ROSIERS	1.522	1.08	0.32	0.39	0.34	1.97a
E6 (18)	ST JEAN DE CHERBOURG	0.573	0.57	-1.32	-0.43	-0.26	0.79
SW1 (19)	WRIGHT	-0.46	0.51	2.16 ^a	0.50	-2.76 ^a	-2.27 ^a
SW2 (20)	ANGERS	0.74	1.76 ^b	3.15 ^a	1.99 ^a	-2.94 ^a	-0.69
SW3 (21)	LACHUTE	4.03 ^a	2.49 ^a	3.99 ^a	2.58 ^a	0.78	-0.39

SW4 (22)	COTEAU DU LAC	2.36 ^a	1.00	2.17 ^a	0.38	-0.54	0.60
SW5 (23)	ST CHARLES DE MANDEVILLE	3.86 ^a	-0.29	4.21 ^a	0.72	2.21 ^a	0.33
SW6 (24)	ST ALBAN	4.83 ^a	0.65	1.69 ^b	1.23	-2.27 ^a	-1.06
SW7 (25)	LAC AUX SABLES	-0.64	1.07	0.37	1.20	-2.74 ^a	-1.18
SW8 (26)	STE ANNE DE LA PERADE	4.35 ^a	1.94 ^b	3.24 ^a	2.09 ^a	3.76 ^a	-0.36

Table 4. Years of change for total annual precipitation (v1), maximum annual precipitation (v2) and maximum consecutive wet days (v3).

station	Change between 1965-1975			Change between 1985-1995			Change between 2005-2015			Change elsewhere		
	V1	V2	V3	V1	V2	V3	V1	V2	V3	V1	V2	V3
SE1 (1)	1972	--	--	1990	--	--	2005	2011	2009	--	--	--
SE2 (2)	--	--	1968	--	--	--	--	--	--	--	--	--
SE3 (3)	--	--	--	--	1995	1986 1995	2012	--	--	--	--	--
SE4 (4)	--	--	--	--	--	1982	--	--	2011	--	--	--
SE5 (5)	--	--	--	--	--	1992	2012	2010	2011	--	1956	--
SE6 (6)	1975	--	--	--	--	1983	--	2013	--	1981	--	--
SE7 (7)	--	--	1976	--	--	--	--	--	2005 2012	--	--	--
SE8 (8)	1977		1970	--	--	--	2001 2009	2013	2014	--	--	--
SE9 (9)	1972	--	1978	--	--	1983	--	--	--	--	--	--
SE10 (10)	1971	1973	1986	--	1984	1996	--	--	2008	--	--	--
SE11 (11)	1974	--	--	--	--	--	2005	--	--	--	--	--
E1 (12)	--	--	--	--	--	1999	2012	--	--	--	--	--
E2 (13)	--	--	--	--	--	--	--	2006	--	--	--	1953
E3 (14)	1978	--	--	--	--	--	--	2004	2011	--	--	--
E4 (15)	--	--	--	--	--	--	--	--	--	--	--	--

E5 (16)	--	--	--	1984	--	--	--	--	2005	2001	--	--
E6 (17)	1977	--	--	1982	--	--	2010	2008	2015	--	--	--
SW1 (18)	--	--	1972	--	--	1998	--	--	--	--	--	--
SW2 (19)	--	--	1968	--	--	1989	--	--	2006	--	--	--
SW3 (20)	--	--	1971	--	--	--	--	--	--	--	--	--
SW4 (21)	1975	--	1973	--	1995	1993	--	--	--	--	--	--
SW5 (22)	--	--	1967	--	1991	1997	--	--	2003	1931	1934	--
SW6 (23)	--	--	--	--	--	--	--	--	2014	--	--	--
SW7 (24)	--	--	1971	--	--	1997	--	--	2008	--	--	--
SW8 (25)	--	--	1964	--	--	--	--	2010	--	--	--	1981

LIST OF FIGURES

FIGURE 1. GEOGRAPHICAL LOCATION OF THE METEOROLOGICAL STATIONS.....	62
FIGURE 2. PEARSON'S TAU COEFFICIENTS OF CORRELATION BETWEEN THE TOTAL ANNUAL PRECIPITATION AND THE AO AND NAOJ INDICES.....	63
FIGURE 3. PEARSON'S TAU COEFFICIENTS OF CORRELATION BETWEEN THE MAXIMUM ANNUAL PRECIPITATION AND THE TNA AND NAOJ INDICES.....	64
FIGURE 4. CWTs OF TOTAL ANNUAL PRECIPITATION IN LINGWICK STATION (A), ST CHARLES DE MANEDVILLE (B) AND ST JEAN DE CHERBOURG (C).....	65
FIGURE 5. CWTs OF MAXIMUM ANNUAL PRECIPITATION IN LINGWICK STATION (A), ST CHARLES DE MANEDVILLE (B) AND ST JEAN DE CHERBOURG (C).....	66
FIGURE 6. CWTs OF AO INDEX (A, B, C), NAOJ INDEX (D, E, F) AND TNA INDEX (G, H, I).....	67
FIGURE 7. ANALYSIS OF XWT RELATIONSHIPS BETWEEN ANNUAL TIME SERIES AND THE AO AND NAOJ INDICES.	68
FIGURE 8. ANALYSIS OF XWT RELATIONSHIPS BETWEEN MAXIMUM TIME SERIES AND THE TNA AND NAOJ INDICES.	69
FIGURE 9. WTC ANALYSES BETWEEN TOTAL ANNUAL PRECIPITATION SERIES AND AO INDEX.	70
FIGURE 10. WTC ANALYSES BETWEEN TOTAL ANNUAL PRECIPITATION SERIES AND NAOJ INDEX.	71
FIGURE 11.. WTC ANALYSES BETWEEN MAXIMUM ANNUAL PRECIPITATION SERIES AND NAOJ INDEX.....	72
FIGURE 12. WTC ANALYSES BETWEEN MAXIMUM ANNUAL PRECIPITATION SERIES AND TNA INDEX	73

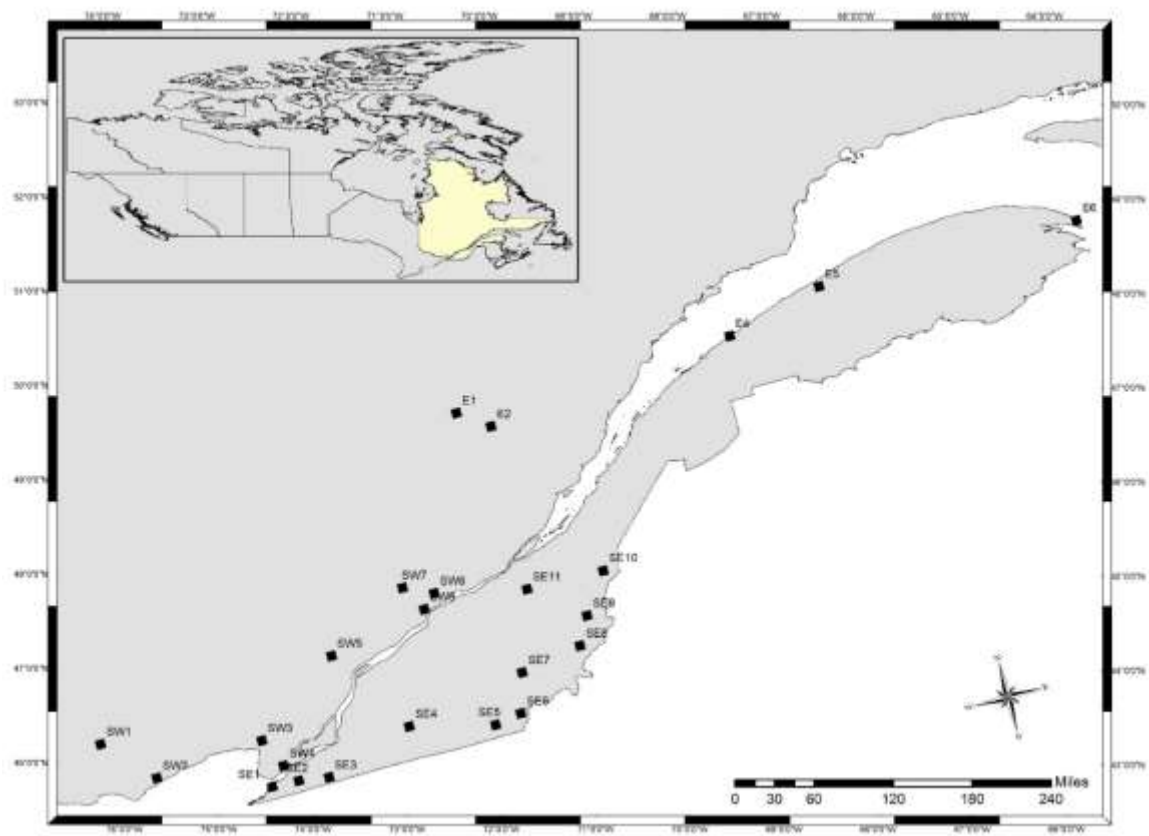


Figure 1. Geographical location of the meteorological stations.

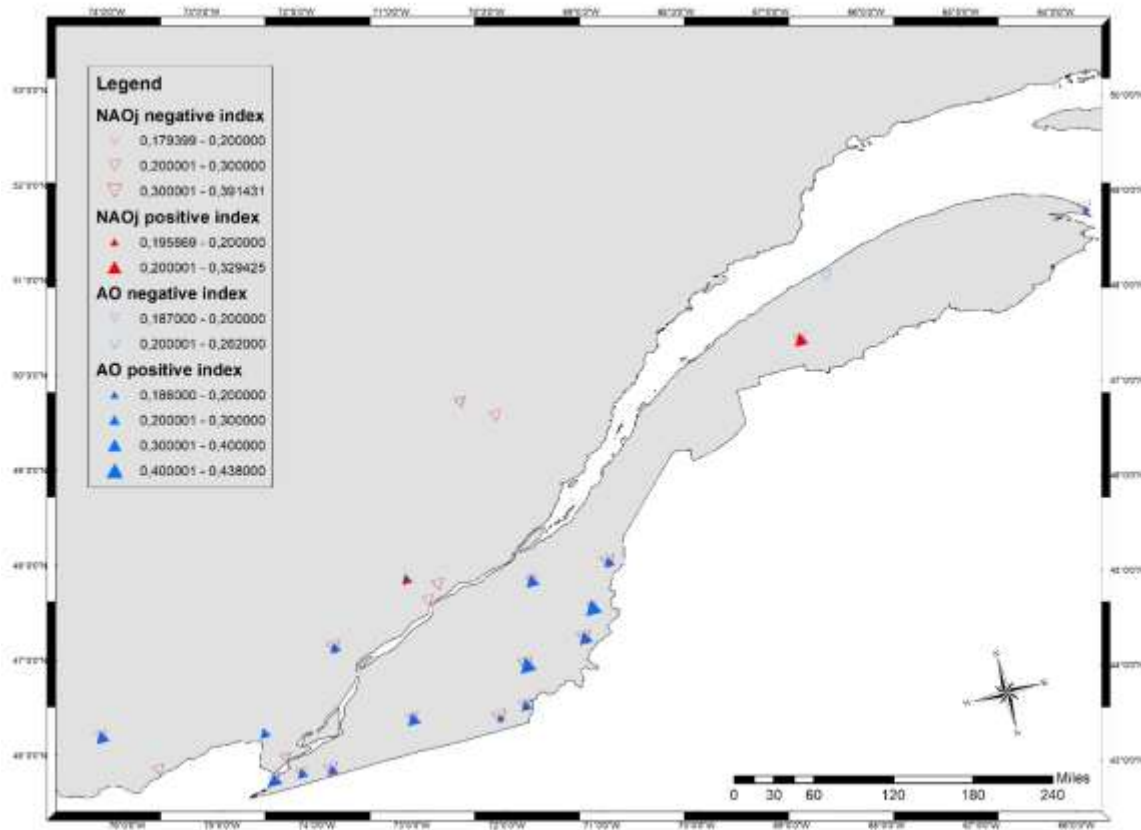


Figure 2. Pearson's coefficients of correlation between the total annual precipitation and the AO and NAOj indices.

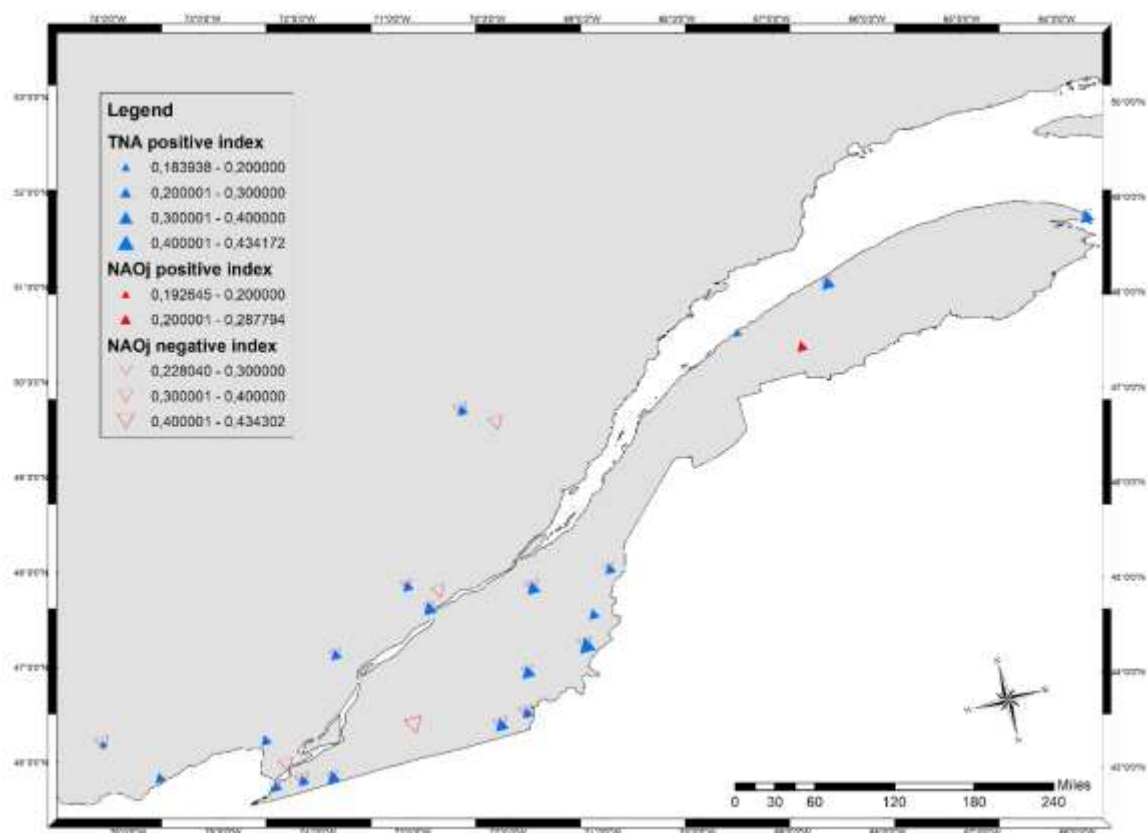


Figure 3. Pearson's coefficients of correlation between the Maximum annual precipitation and the TNA and NAOj indices.

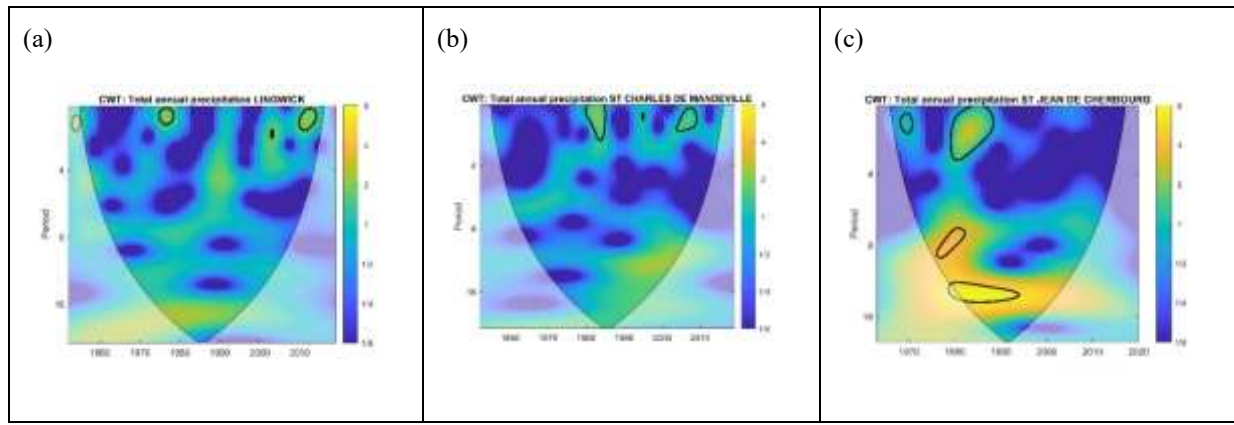


Figure 4. CWTs of total annual precipitation in Lingwick station (a), St Charles de Manedville (b) and St Jean de Cherbourg (c).

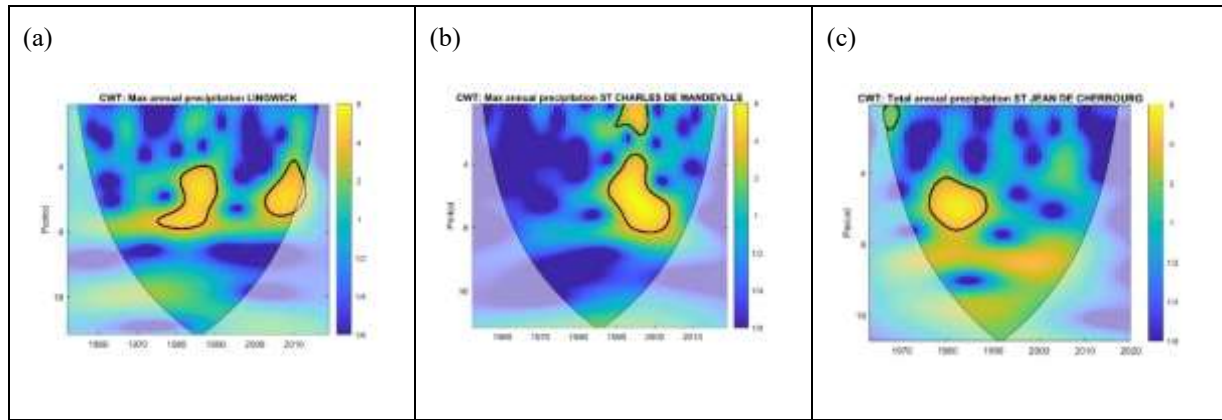


Figure 5. CWTs of maximum annual precipitation in Lingwick station (a), St Charles de Manedville (b) and St Jean de Cherbourg (c).

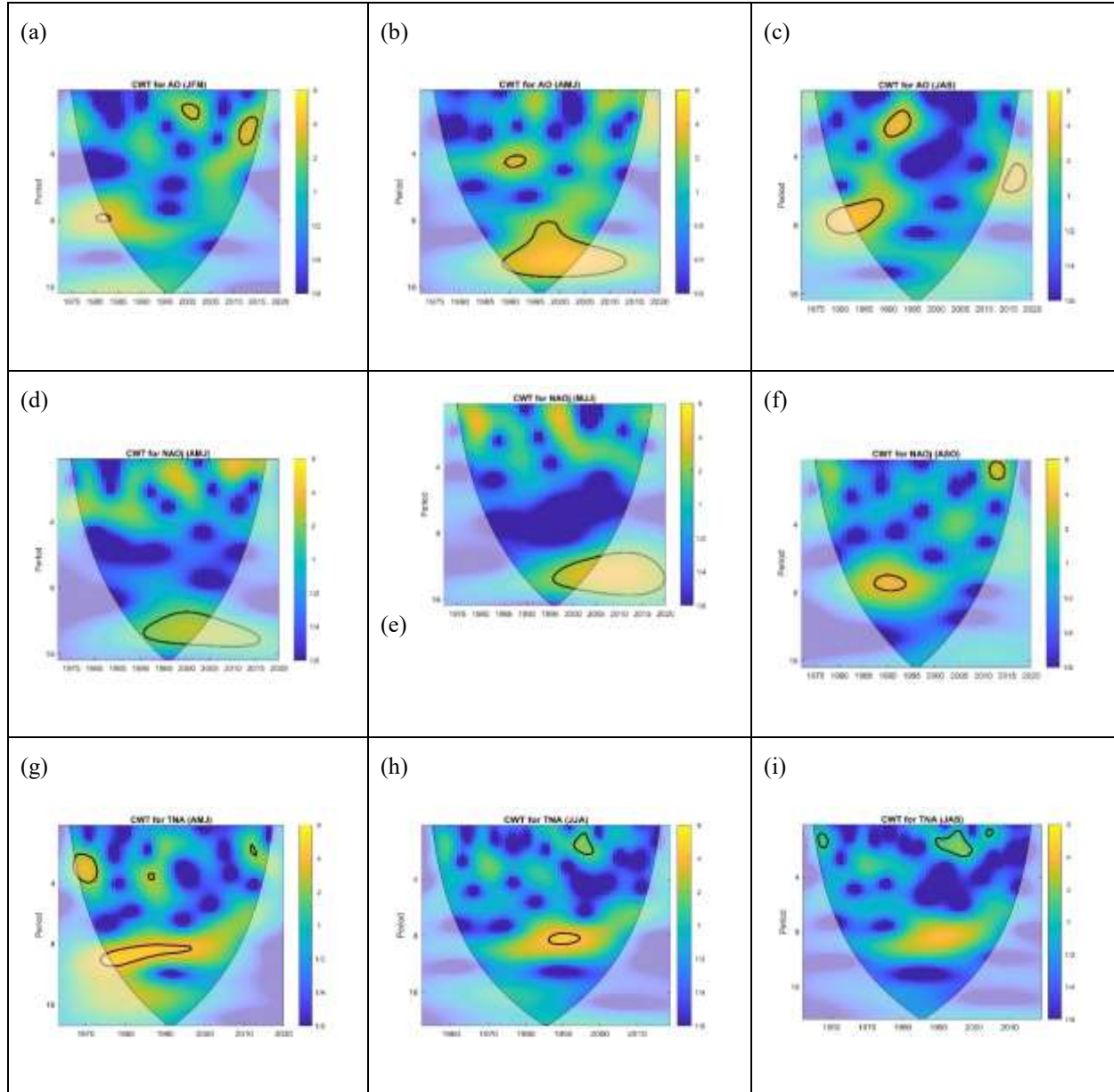


Figure 6. CWTs of AO index (a, b, c), NAOj index (d, e, f) and TNA index (g, h, i)

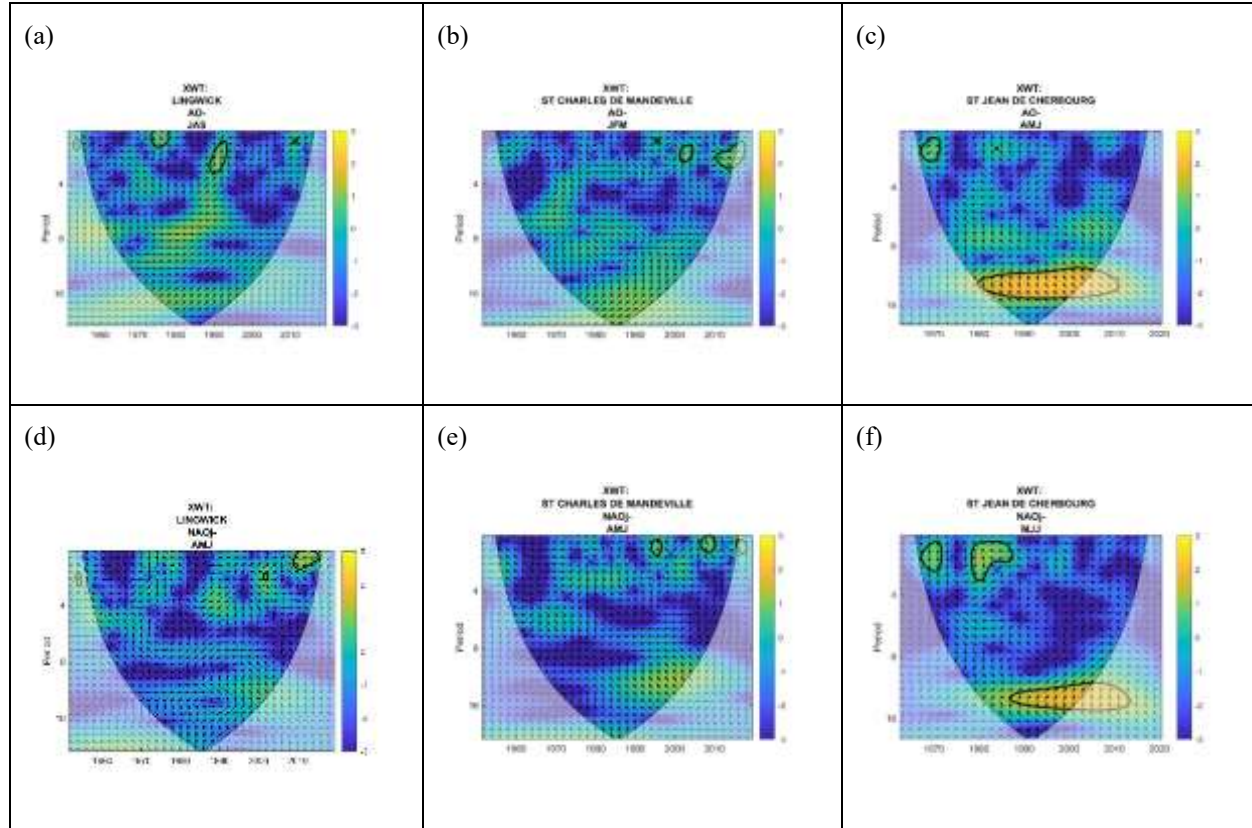


Figure 7. Analysis of XWT relationships between annual time series at the selected stations and the AO and NAOj indices during the months of significant correlation.

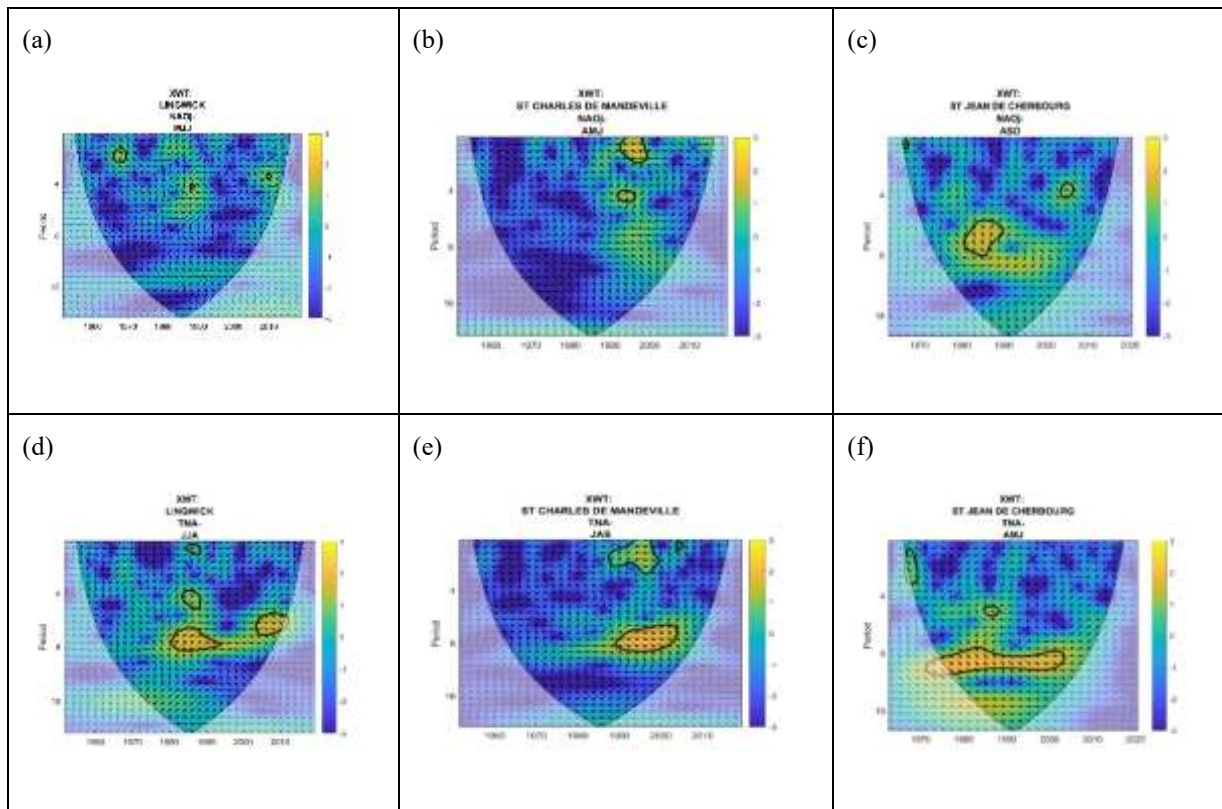


Figure 8. Analysis of XWT relationships between maximum time series at the selected stations and the TNA and NAOj indices during the months of significant correlation.

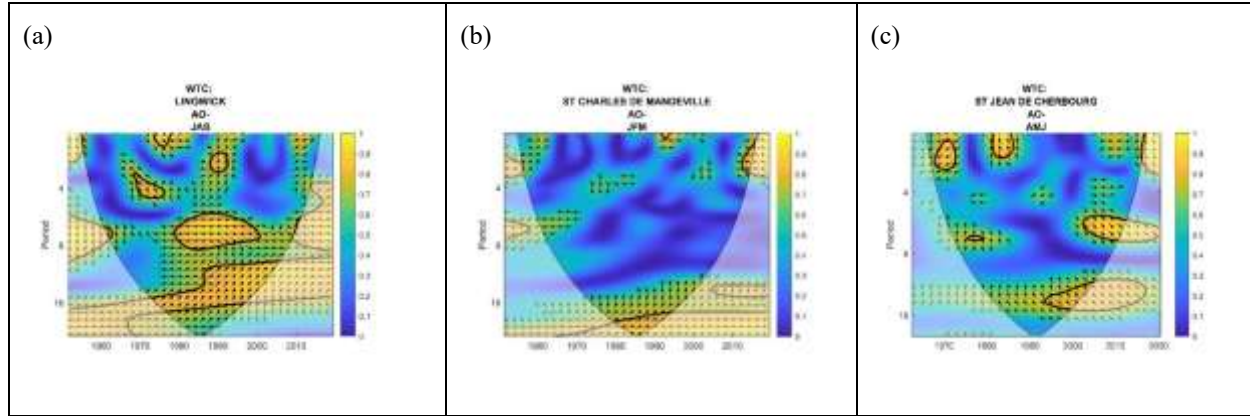


Figure 9. WTC analyses between total annual precipitation series at the selected stations and AO index during the months of significant correlation.

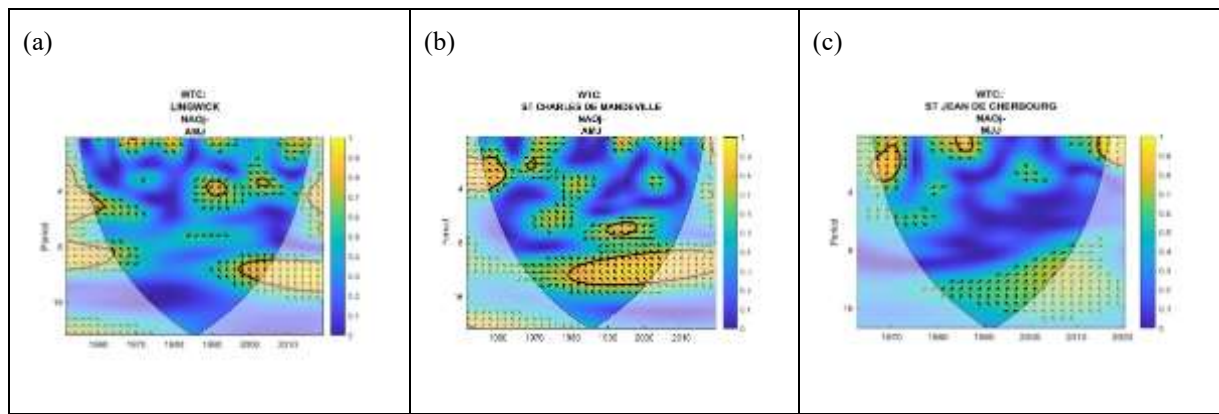


Figure 10. WTC analyses between total annual precipitation series at the selected stations and NAOj index during the months of significant correlation.

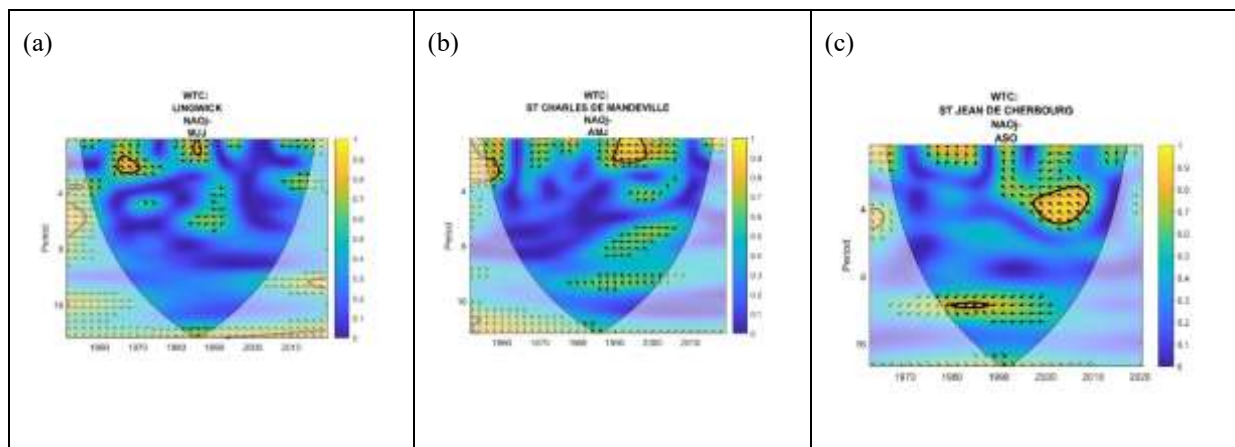


Figure 11. . WTC analyses between maximum annual precipitation series at the selected stations and NAOj index during the months of significant correlation.

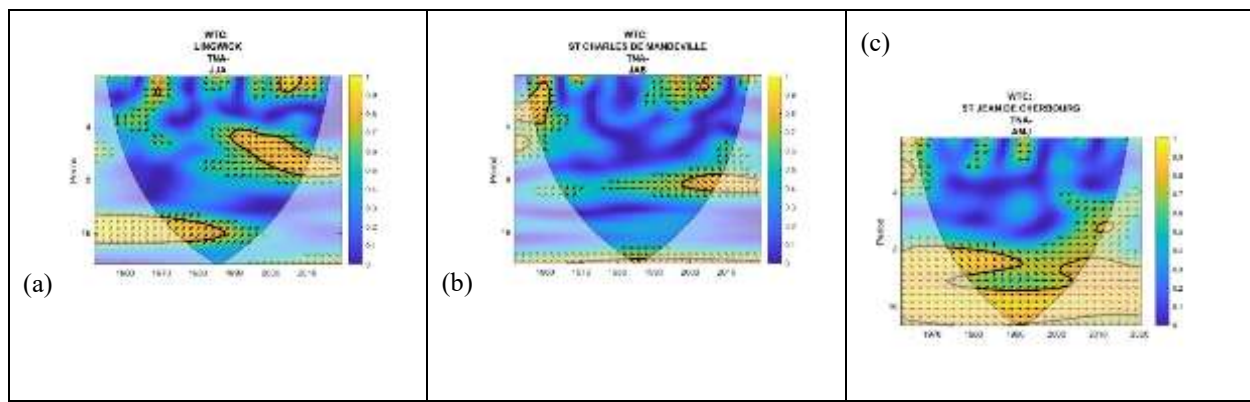


Figure 12. WTC analyses between maximum annual precipitation series at the selected stations and TNA index during the months of significant correlation.

